

**University of Alberta**

**Cell adhesion and viability in HUVEC monolayers after low temperature exposure**

**By**

**Kristine Michelle Kluthe** ©

**A thesis submitted to the Faculty of Graduate Studies and Research in partial  
fulfillment of the requirements for the degree of Master of Science**

**in**

**Medical Sciences – Laboratory Medicine and Pathology**

**Edmonton, Alberta**

**Fall 2007**



Library and  
Archives Canada

Bibliothèque et  
Archives Canada

Published Heritage  
Branch

Direction du  
Patrimoine de l'édition

395 Wellington Street  
Ottawa ON K1A 0N4  
Canada

395, rue Wellington  
Ottawa ON K1A 0N4  
Canada

*Your file* *Votre référence*  
*ISBN: 978-0-494-33282-5*  
*Our file* *Notre référence*  
*ISBN: 978-0-494-33282-5*

#### NOTICE:

The author has granted a non-exclusive license allowing Library and Archives Canada to reproduce, publish, archive, preserve, conserve, communicate to the public by telecommunication or on the Internet, loan, distribute and sell theses worldwide, for commercial or non-commercial purposes, in microform, paper, electronic and/or any other formats.

The author retains copyright ownership and moral rights in this thesis. Neither the thesis nor substantial extracts from it may be printed or otherwise reproduced without the author's permission.

#### AVIS:

L'auteur a accordé une licence non exclusive permettant à la Bibliothèque et Archives Canada de reproduire, publier, archiver, sauvegarder, conserver, transmettre au public par télécommunication ou par l'Internet, prêter, distribuer et vendre des thèses partout dans le monde, à des fins commerciales ou autres, sur support microforme, papier, électronique et/ou autres formats.

L'auteur conserve la propriété du droit d'auteur et des droits moraux qui protègent cette thèse. Ni la thèse ni des extraits substantiels de celle-ci ne doivent être imprimés ou autrement reproduits sans son autorisation.

---

In compliance with the Canadian Privacy Act some supporting forms may have been removed from this thesis.

Conformément à la loi canadienne sur la protection de la vie privée, quelques formulaires secondaires ont été enlevés de cette thèse.

While these forms may be included in the document page count, their removal does not represent any loss of content from the thesis.

Bien que ces formulaires aient inclus dans la pagination, il n'y aura aucun contenu manquant.

  
**Canada**

## **Abstract**

It is widely known in the field of cryobiology that the primary limiting factor in applications of cell and tissue cryopreservation is the post-thaw recovery of function and viability. A limiting factor in the cryopreservation of corneas and cardiovascular tissue is cryoinjury to endothelial monolayers. To determine a cellular monolayer response to freezing conditions, Human Umbilical Vein Endothelial Cells (HUVEC) were grown to confluence and exposed to a graded freezing protocol with and without dimethylsulfoxide. Conditions leading to cell death and detachment were identified. It was concluded that factors leading to death or detachment were independent and indicating that separate cryopreservation techniques may be required to protect viability and adhesion.

## Acknowledgements

To my Mom, Dad and Nolan - Thank you for putting up with my science chatter and for being excited about my research even when you didn't have a clue exactly what I was doing. You encouraged me to keep going when things were tough and taught me to never quit.

To Dr. Locksley McGann – Thank you for not only being my supervisor but for truly being my mentor and friend. Without your support and encouragement this thesis would not have been possible. Thank you for recognizing my dreams and allowing me the freedom to pursue them while still encouraging me all the way.

To Dr. Janet Elliott – Thank you also for your support, encouragement and empowerment. You showed me that a strong professional woman can still have it all.

To my friends – Thank you for continuing to support me and lend an ear when I just needed to vent. I will always appreciate your love and support.

## Table of Contents

### Chapter 1

<u>Introduction</u>	Page 1
Principles of Cryopreservation	Page 1
Singe Cell and Tissue Preservation	Page 7
A Review of Monolayer Preservation	Page 8
Implications of Vascular and Corneal Preservation	Page 9
Cellular Adhesion and Implications for Cryopreservation	Page 10
Experimental Motivation	Page 12
Objectives of This Thesis	Page 13

### Chapter 2 – Assessment Techniques for Cell Monolayers

<u>Introduction</u>	Page 15
SYTO/EB Cell Staining	Page 16
Quality Image Capture	Page 17
Image Analysis Software	Page 18
Manual Justification of Cell Counting Software	Page 20
Qualitative Justification of Cell Density as an Indicator of Adhesion	Page 21
<u>Discussion</u>	Page 24
<u>Conclusion</u>	Page 25

### Chapter 3 – Optimal HUVEC Growth Curve Conditions and Quantitative Confluence Analysis

<u>Introduction</u>	Page 26
Determination of Confluence	Page 27
<u>Materials and Methods</u>	
HUVEC Cell Culture	Page 28
Fibronectin Concentration	Page 29
Growth Curve	Page 30
Growth Curve Analysis	Page 31
<u>Results</u>	
Optimal Fibronectin Concentration	Page 31
Growth Curve and Quantitative Determination of Confluence	Page 32
<u>Discussion</u>	Page 37
<u>Conclusion</u>	Page 39

### Chapter 4 – The Cryopreservation of Confluent HUVEC Monolayers with and Without 1M DMSO

<u>Introduction</u>	Page 40
<u>Materials and Methods</u>	
The Experimental System	Page 42
Thermal Characteristics of the System	Page 42
HUVEC Cell Preparation	Page 43

Graded Freezing Protocol	Page 43
<u>Results</u>	
Thermal Characteristics of the System	Page 45
Adhesion and Viability of HUVEC Monolayers Following Graded Freezing	Page 47
<u>Discussion</u>	
Thermal Characteristics of the System	Page 51
HUVEC Monolayer Response to Freezing	Page 51
Insight Gained from a Graded Freezing Protocol	Page 53
The Effectiveness of DMSO as a HUVEC Monolayer Cryoprotectant	Page 54
Hypothesis Related to Cellular Adhesion	Page 56
<u>Conclusion</u>	Page 57
<b><u>Chapter 5 – Influence of Prior Osmotic Shrinkage on Graded Freezing Response</u></b>	
<u>Introduction</u>	Page 59
<u>Materials and Methods</u>	
Cell Preparation	Page 61
Condition Screening Experiment	Page 61
Prior Hypertonic Exposure in 2x PBS	Page 62
<u>Results</u>	
Condition Screening Experiment	Page 63
Cellular Viability and Adhesion Following 2x PBS Exposure	Page 65
<u>Discussion</u>	Page 67
<u>Conclusion</u>	Page 70
<b><u>Chapter 6 – General Conclusions</u></b>	
<u>Experimental Conclusions</u>	Page 71
<u>Limitations of Research</u>	Page 76
<u>Future Research</u>	Page 76
<b><u>References Cited</u></b>	<b>Page 78</b>

## List of Figures

### **Chapter 1 – Introduction**

#### **Figure 1**

Simulation of cell size after addition and dilution of a permeant cryoprotectant \_\_\_\_\_ Page 6

### **Chapter 2 - Assessment Techniques for Cell Monolayers**

#### **Figure 1**

Examples of fluorescent nuclei in cells stained with SYTO/EB showing live green cells, dead (red) cells and patterns of detachment indicated by black areas between green and red cells \_\_\_\_\_ Page 17

#### **Figure 2**

Representative images of overexposed and properly exposed images, indicating the yellow color distribution in the overexposed image \_\_\_\_\_ Page 18

#### **Figure 3**

Interface of Viability 3 program \_\_\_\_\_ Page 19

#### **Figure 4**

Representation of absolute versus relative viability \_\_\_\_\_ Page 20

#### **Figure 5**

Cell adhesion grading scheme \_\_\_\_\_ Page 22

#### **Figure 6.**

Assessment of adhesion comparing the quantitatively determined cell density using Viability 3, to the qualitatively assigned adhesion grading \_\_\_\_\_ Page 23

#### **Figure 7.**

Loss of adhesion and patchiness \_\_\_\_\_ Page 24

### **Chapter 3 – Optimal HUVEC Growth Curve Conditions and Quantitative**

#### **Confluence Analysis**

#### **Figure 1.**

A typical cell growth curve indicating the lag phase, the exponential phase of cell growth, the confluent or stationary phase and the death phase \_\_\_\_\_ Page 27

Figure 2.

Diagrammatic representation of fibronectin concentration  
experimental methods \_\_\_\_\_ Page 29

Figure 3.

Diagrammatic representation of growth curve experimental methods \_\_\_\_\_ Page 30

Figure 4.

Cell density after 48 hrs of cell culture as a function of fibronectin  
coating concentration \_\_\_\_\_ Page 32

Figure 5.

HUVEC growth curve over a 14 day period \_\_\_\_\_ Page 33

Figure 6.

Phase contrast images of HUVEC growth curve indicating increasing cell density and  
changes in cell morphology \_\_\_\_\_ Page 34

Figure 7.

SYTO/EB stained HUVEC growth curve images indicating increasing  
cell density and viability \_\_\_\_\_ Page 36

Figure 8.

Growth curve highlighting the experimentally determined growth time selected for  
confluent monolayers to be used in further experiments \_\_\_\_\_ Page 37

**Chapter 4 – The Cryopreservation of Confluent HUVEC Monolayers With and  
Without 1M DMSO**

Figure 1.

Schematic diagram of the experimental system \_\_\_\_\_ Page 42

Figure 2.

Schematic diagram of graded freezing protocol \_\_\_\_\_ Page 44

Figure 3.

Representative recorded temperature profile with 1.5 mL media in 20 mL  
scintillation vials placed in a methanol bath at -5 °C \_\_\_\_\_ Page 46

Figure 4.

Absolute viability and adhesion for HUVEC monolayers after direct thaw from different experimental temperatures in the graded freezing procedure \_\_\_\_\_ Page 47

Figure 5.

Absolute viability and adhesion for HUVEC monolayers after plunge from different experimental temperatures in the graded freezing procedure \_\_\_\_\_ Page 48

Figure 6.

Results for 1M DMSO in direct thaw and plunge conditions \_\_\_\_\_ Page 49

Figure 7.

Images representative of increased cellular adhesion in samples plunged to -196 °C and direct thaw samples for experimental temperatures below -25 °C \_\_\_\_\_ Page 50

**Chapter 5 – Influence of Prior Osmotic Shrinking on Graded Freezing Response**

Figure 1.

Schematic diagram of conditions screening experiment \_\_\_\_\_ Page 62

Figure 2.

Schematic diagram of pre-shrinkage in 2x PBS prior to graded freezing protocol \_\_\_\_\_ Page 63

Figure 3.

Graded freezing validation experiment using a direct thaw from -10 °C for various experimental conditions \_\_\_\_\_ Page 64

Figure 4.

Comparison of viability following graded freezing direct thaw of short and long hold pre-shrinkage in 2x PBS with 1M DMSO and no-DMSO, DMSO alone, and no-DMSO treated samples \_\_\_\_\_ Page 66

Figure 5.

Comparison of adhesion following graded freezing direct thaw of short and long hold pre-shrinkage in 2x PBS with 1M DMSO and no-DMSO, DMSO alone, and no-DMSO treated samples \_\_\_\_\_ Page 67

## **Chapter 1 – Introduction**

While successful organ and tissue preservation is the ultimate goal of many medical researchers, the target appears a long way from reality. Currently the limits of successful preservation extend only to single cells in suspension such as sperm, blood components, and hematopoietic stem cells, with very limited success in multi-cellular tissues. The ability to successfully preserve cells and tissues spans an important range of applications from agriculture to medicine. Within transplant medicine, the establishment of tissue banks ensures there is an adequate organ and tissue supply to meet the increasing health care demands. More specifically, the ability to bank corneas, skin, cardiovascular tissue, and vascular tissue, would allow patients to be properly matched, reduce the risk of rejection, allow quicker delivery of the transplant and reduce waiting lists. Preservation of such tissues also allows expansion of geographical regions that can be served by a native tissue pool, thereby treating more patients and reducing corresponding health care costs (1). Tissue banks will also be required for preservation and storage of biomaterials, to maintain large stocks in order to ensure a steady supply and meet the unpredictable demand for specific tissues in the clinical setting (2). In addition, advances in tissue bioengineering and biosynthetic tissue development will also increase the demand and require the ability to store prior to distribution (3). Simple preservation techniques such as refrigeration or tissue culture are limiting due to restricted shelf life, the high cost and risk of contamination or genetic drift (2). Therefore, there is a need to develop proper preservation techniques as structural tissues, whose function depends to a large extent on the properties and functional abilities of the extracellular matrix, are shown to be more prone to post-transplantation complication and failure if the cell population is non-viable (2).

### **Principles of Cryopreservation**

Before a successful preservation technique can be developed, a firm grasp on the principles of cryopreservation is required. The formation of ice and the corresponding cellular response to this process are fundamental concepts. Around  $-0.6^{\circ}\text{C}$ , biological water in isotonic conditions becomes thermodynamically metastable and favors a

crystalline state, producing ice (2). The ice crystal will continue to grow as water molecules leave the random liquid phase and join the fixed ice crystal lattice (4). This process is important as the ice-water transition phase is critical to cryopreservation (2). However, as the pure liquid is cooled it does not necessarily form ice crystals spontaneously. The presence of a seed crystal or nucleating event is required to trigger a phase transition (4). Nucleation is the stochastic aggregation of water molecules into clusters large enough for ice crystals to grow (4). Ice can be nucleated in a supercooled sample, with supercooling defined as the difference in temperature between the melting point of a solution and its actual temperature (4). Therefore, the rate of crystallization depends on the kinetics of nucleation and subsequent crystal growth, both of which slow down if the viscosity of the solution increases as occurs with decreasing temperature (2). As ice grows within the sample, the pure water molecules leave the extracellular solution, excluding solutes from the growing ice lattice resulting in the unfrozen fraction becoming increasingly concentrated (2, 4). As the cell membrane is semi-permeable, water is able to pass across the membrane in response to the increasingly concentrated extracellular environment. For a cell in this freezing solution, a chemical potential imbalance occurs between the intracellular environment and the external unfrozen solution, increasing the flow of water out of the cell and the diffusion of solutes into the cell (2). The rate of water efflux from the cell is proportional to the magnitude of the driving force or osmotic pressure, the hydraulic conductivity ( $L_p$ ) (permeability to water of the plasma membrane) and the surface area to volume ratio (2, 5).

$$\frac{dV}{dt} = L_p A R T (\pi_i - \pi_e)$$

Equation 1. Where V is the volume, t is time, A is surface area, R is the universal gas constant, T is the absolute temperature in Kelvin and  $\pi$  is osmolality where subscript (i) is internal and (e) is external to the cell (6, 7)

It is thought that water moves across the membrane by either aquaporins or diffusion dependant on the fluidity of the lipid bilayer; however, both are temperature dependant (8). An Arrhenius temperature dependence with the use of activation energy,  $E_a$ , is used to describe the temperature dependence of hydraulic conductivity (9).

$$L_p = K * \exp \left( \frac{-E_a}{RT} \right)$$

Equation 2. Where K is a fitting constant.

Hydraulic conductivity and its activation energy values are unique for each cell type. Since freezing and thawing introduce such large changes in the osmotic environment of cells,  $L_p$  and  $E_a$  are the most important parameters for determining a given cell types' response to low temperature exposure (4).

Developed by Mazur, the current freezing injury model most accepted by researchers is known as the 2-factor hypothesis which describes unique mechanisms of injury during rapid or slow cooling (10). Rapid cooling will produce ice in the extracellular solution more rapidly than the cell can adapt by losing intracellular water, therefore increasing the osmolality gradient across the plasma membrane as the solution is cooled (10). The cytoplasm within the cell becomes increasingly supercooled and intracellular ice nucleation becomes increasingly likely, the likelihood increasing with the amount of supercooling (4). Water remaining within the cells undergoes intracellular freezing, producing intracellular ice which has been associated with lethal cell injury under most conditions (2). Possible sites and mechanisms of cell injury have been proposed to include the plasma membrane or membranes of intracellular organelles, non-mechanical damage thought to be gas bubble formation by intracellular ice, or osmotic effects due to melting of intracellular ice during warming (11-16).

In contrast, slow cooling allows the cell to remain close to osmotic equilibrium as water diffuses from the cell at the same rate as pure water is lost from the extracellular solution due to ice formation (4). Cell injury during slow cooling occurs as a result of increased intra-and extracellular osmolality created by the extracellular hypertonic environment which results in osmotic shrinkage. Unlike rapid cooling, during slow cooling there is low supercooling and no intracellular freezing. Damage is thought to be related to exposure to high concentrations of intracellular and extracellular solutes or to mechanical interactions between cells and the extracellular ice (2).

Several theories regarding cell damage resulting from slow cooling exist. Meryman proposed a minimum cell volume hypothesis which states that membrane damage results from "osmotic stresses" due to increased extracellular solute concentrations imposed on the cell membrane when the cell volume is decreased beyond

a minimum tolerable size (17). It was suggested freezing injury in red blood cells and likely most other cell types is unrelated to any absolute concentration of any particular solute (17). Instead this theory proposes that injury is related to the removal of a critical proportion of the total cell water and the associated reduction in cell size beyond a critical volume (17). If cells cannot shrink freely in response to the concentration gradient, then osmotic pressure gradients develop across the plasma membrane; as these differences exceed the tolerance of the membrane, irreversible changes in membrane permeability result in membrane damage (17, 18). Another theory proposed by Lovelock suggested dilution stress and exposure to high salt concentrations are responsible for cellular damage (19). Exposure to salt concentrations greater than 0.8 M renders cells sensitive when exposed to a subsequent thermal or mechanical shock (19). Alternatively, higher salt concentrations greater than 3.0 M were found to cause complete destruction of the cellular membrane and it was hypothesized that salt has a lyotropic effect on the cell membrane (19).

Regardless of the mechanisms of cellular injury described by the 2-factor hypothesis, avoidance of slow-cool and rapid-cool injury is dependant on cooling rate. An optimal cooling rate is an intermediate rate that minimizes cellular damage by trading off between slow-cool and rapid-cool induced damage thereby avoiding excessive cell shrinkage and intracellular ice formation. Each cell type will have an individual optimal cooling rate based on its unique  $L_p$  and  $E_a$ . These characteristics indicate that an optimal preservation protocol must be individually determined for each cell type.

In an effort to develop optimal freezing protocols, supplements referred to as cryoprotective agents (CPAs), are used to reduce the cooling stress imposed on the cell during freezing. There are two categories of CPA's: permeating and non-permeating. Permeating cryoprotectants include dimethyl sulphoxide, glycerol and 1,2-propanediol, which are capable of passing through the cellular membrane. Non-permeating cryoprotectants include polymers such as polyvinyl pyrrolidone, hydroxyethyl starch and various sugars which do not readily cross the plasma membrane. Permeating CPAs act primarily to reduce cell injury on a colligative basis by lowering the vapor pressure of the aqueous solution, thereby reducing the amount of ice formed so that solute concentrations and the resulting reduction in cell volume are insufficient to exceed the tolerance of the

cell (17). In high concentrations CPAs increase the viscosity of the intra- and extracellular solutions and reduce the amount of ice formation by affecting the rate of nucleation and ice crystal growth (2). However, the addition of permeating and non-permeating cryoprotectants causes the cells to undergo potentially damaging volume excursions. Observations have noted shrinking below tolerated osmotic limits upon addition and swelling above critical limits upon dilution depend on temperature and solute concentration (20). An example of volume change in bovine chondrocyte cells is illustrated in Figure 1. Cell size decreases upon addition of DMSO as intracellular water leaves the cell to equilibrate the concentration gradient across the membrane. As DMSO permeates the cell, extracellular water follows, increasing cell volume until concentration equilibrium is reached. Upon dilution extracellular water enters the cell to equilibrate the excessive DMSO concentration intracellularly, but subsequently volume reduces as DMSO leaves the cell, equilibrating its concentration gradient across the membrane. Both the addition and dilution of CPAs are temperature dependent as a result of the temperature dependence of  $L_p$  and  $E_a$ .

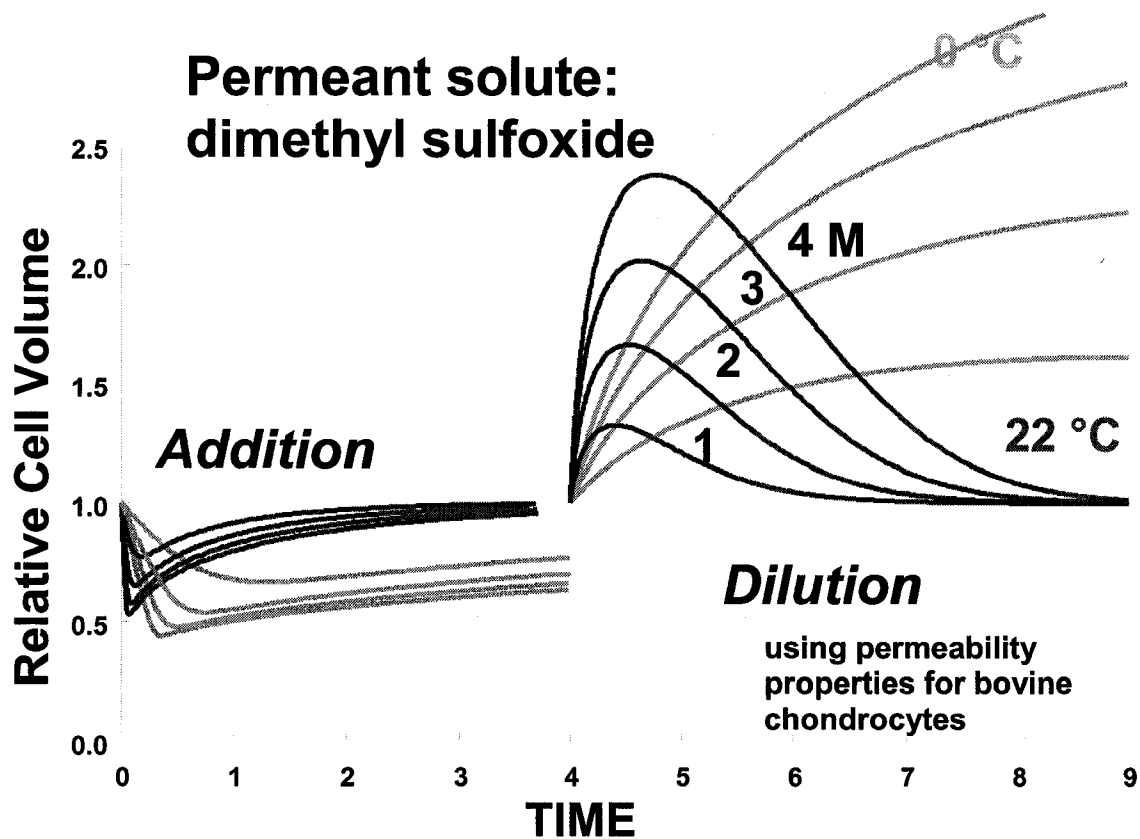


Figure 1. Simulation of cell size after addition and dilution of a permeant cryoprotectant. Image used with permission from Locksley McGann.

Computer-generated simulations using corneal endothelial cells show 1M DMSO is tolerated in a single step procedure but 2 M exceeds the tolerated limits causing volume excursions to approximately 140% of isotonic volume (20). Slow cool injury can be reduced by adding these low molecular weight agents that function by colligatively reducing the salt concentration in the frozen solution at subzero temperatures (21). They delay cell exposure to toxic concentrations of extracellular salts at lower temperatures and minimize cell volume excursions therefore reducing cellular sensitivity to thermal or mechanical shock and prevent the cell from reaching the minimal critical volume (21). The use of CPAs allows for the successful preservation of some single cell types in suspension.

## **Single Cell and Tissue Preservation**

The preservation of single cells in suspension is not without complications or limitation. Stresses imposed on the cell during freezing include: intra-and extracellular ice formation, cellular dehydration, increases in viscosity, and solute and ionic concentrations; all of which contribute to some form of cell damage (22). Considerable evidence suggests that the primary site of cell injury is the plasma membrane (18).

However, the preservation of tissues is substantially more complicated and several other limitations restrict the ability to successfully preserve. Tissues are complex systems of organized cells which require coordinated interactions between adjacent cells and the extracellular matrix for normal cellular function (23). It has been suggested that difficulties in tissue preservation are due to structural organization within tissue (24). Within multi-cell-layer tissues, limitations exist which are non-existent for single cell suspensions. The time required for diffusion of cryoprotectants to the interior of the tissue potentially over exposes the cells at the surface to the toxicity of CPAs (2). Large thermal gradients from the surface to the interior of the tissue may exist, resulting in non-uniform cooling rates throughout the tissue (2). These thermal gradients also have the potential to induce mechanical stress due to uneven expansion or contraction of the biomaterial (2). In addition, optimal cooling rates in multi-cell-type tissues are difficult to define and achieve as optimal survival varies by several orders of magnitude between different cell types, based on their individual  $E_a$  and  $L_p$  (2). As well, cell-cell junctions have been suggested as potential targets of injury during tissue preservation (2). Confirming these limitations, a study compared the cryopreservation of suspensions and monolayer cell preparations of corneal keratocytes and found the optimal cooling rate resulting in cell preservation was different between suspension and adherent cells (25). For cooling at 1°C/min it was reported that 80% of suspension cells survived with 10% propane-1,2-diol (PROH), compared to only 25% of cells in a monolayer (25). However, when cooling at 0.2 °C/min, 80% of monolayer cells survived compared to only 50% of cells in suspension (25). These findings indicate that the optimum rate of cell cooling is different for monolayers but tolerance to factors which cause slow cool injury is increased, possibly related to the presence of gap junctions (25, 26).

## **A Review of Monolayer Preservation**

A clear understanding of cellular adhesion and viability of a monolayer in response to freezing will provide researchers with the knowledge to preserve tissues such as vessels and corneas. However, before the successful preservation of tissues is achieved it is important to understand that there are limitations to the preservation of single cells, to which monolayers add an increased level of complexity. To investigate the differences between single cells and monolayers, one study compared cellular response to freezing in suspension and in monolayers attached to glass using Madine – Darby Canine Kidney (MDCK) cells which form intracellular junctions and V-79 Chinese Hamster cells which do not form intracellular junctions (27). Cell suspensions and monolayers were frozen to  $-40\text{ }^{\circ}\text{C}$ , followed by re-warming to  $37\text{ }^{\circ}\text{C}$  (27). The results indicated that attached cells are more susceptible to cryoinjury compared to cell suspensions and that cell-cell junctions further decreased the post-freeze recovery potential (27). The authors that proposed the development of cell junctions and the organization of the cytoskeleton were responsible for these observations (27).

An explanation for the limited success in tissue preservation could stem from the fact that current techniques of tissue preservation are essentially extensions of techniques developed for single cell systems (28). It has become clear that these techniques are not based on the understanding of low temperature responses in tissues and organs (37). Features that are unique to monolayers systems such as cell-cell and cell-matrix interactions alter the cryobiological response of cells (29). The basis of interaction between attachment and preservation is not known, and the requirement for attachment may alter the combination of conditions, cryoprotectants and cooling rates required for optimal recovery (29). Studies have found that cells frozen with firm cell-cell contacts may not survive freeze-thaw cycles and are more susceptible to toxic and osmotic effects associated with the addition and removal of cryoprotectants (23, 30). It has also been suggested that cryopreservation may interfere with the attachment mechanisms, leading to detachment causing architectural damage to the tissue (29). Previous studies have investigated the unique response of cell-cell and cell-surface interactions. It is thought that intercellular ice formation and propagation occurs through intercellular junctions. Acker et al., based on their findings for V-79W Chinese hamster fibroblasts grown in

suspension, on glass, in colonies or in spheroids, have found sweeping patterns of intracellular ice formation in cells joined by intracellular junctions (23).

Other studies have investigated tissue response to cryopreservation. Slow thawing has been found to be more successful compared to rapid thawing of common iliac artery (31). Spontaneous fractures have also been found in preserved vessels on thawing or after clinical implantation and endothelium has been found to be dramatically impaired in heart valves upon preservation (32, 33). Several studies have used a variety of preservation protocols in an effort to successfully preserve monolayers and have reported attached cells have higher survival with: slow cooling rates (0.3 °C/min) with 10% dimethyl sulphoxide (DMSO), slow cooling (0.2 °C/min) with 10% propane-1,2-diol (PROH) or slow cooling at 1 °C/min followed by rapid (100 °C/min) or slow (1 °C/min) warming (29, 32, 34). Such variability in cell preservation protocols indicates there is a need to individually determine the best preservation protocol for each cell type.

In an effort to understand the unique response of adherent cells to preservation protocols, several investigators have speculated on mechanisms of damage. These mechanisms include: mechanical stress during shrinkage since adherent cells are allowed to shrink in only one dimension whereas cells in suspension are able to shrink in three dimensions; firm attachment within tissues which does not allow cells to move freely so that the cells may be damaged by the advancing ice front; a restricted osmotic response due to a reduced membrane surface area for osmotic exchange may lead to reduced water efflux and intracellular ice nucleation at higher temperatures; cellular interactions may facilitate the nucleation of intracellular ice (23, 26, 28, 29, 35).

### **Implications of Vascular and Corneal Preservation**

The focus of this research project specifically targeted endothelial monolayer response to freezing injury so that knowledge and insight could be gained towards the successful preservation of corneal and vascular tissue. Currently a limited availability of autologous bypass material and an increasing frequency of re-operation necessitates the use of less satisfactory autologous graft material, requiring arterial substitutes which are being used in vascular reconstructive procedures (32, 36). Therefore the preservation and banking of vascular tissue would ensure an increased and more suitable supply of

vascular tissue. The ability to cryopreserve autologous endothelial cells from umbilical cords would allow for use in older age to prevent thrombosis, degeneration and graft rejection as well as allow the preservation of a unique cell source which is readily available and ethically obtained (36). However, previous attempts at cryopreservation have resulted in freezing injury where endothelial cells within the vessel have become detached from the subendothelial bed, giving rise to large areas lacking endothelium and substantial damage (31, 32, 36). Maintenance of this endothelial layer is essential as it is the key regulator of homeostasis, it continuously interacts with blood components and structures within the vessel itself, and is essential in the maintenance of vessel tone and anti-thrombotic properties (31).

Correspondingly, the human corneal endothelial cell monolayer does not divide to any significant extent after birth, therefore, with age there is a gradual loss of cells (37). When cell density has been reduced beyond a significant level, the endothelium cannot function to maintain corneal clarity and becomes permanently cloudy leading to eventual blindness for which corneal transplant is the only option (37). Tight junctions between endothelial cells in the corneal monolayer are critically important for the maintenance of transparency in the stroma, therefore indicating the need to maintain cellular tight junctions during preservation (38). Similarly to vascular tissue, endothelial cell detachment from the underlying Descemet's membrane and loss of viability are major effects of cellular preservation (3). Endothelial cell survival is the limiting factor of cryopreservation and a good predictor of the applicability of the cornea transplants (34, 39). Limited success has been achieved with past studies where classical cryopreservation protocols were applied to corneas (3).

### **Cellular Adhesion and Implications for Cryopreservation**

Cell-to-cell and cell-surface interaction are essential to the proper functioning of a monolayer system. Integrins are known to be the primary mediators of cell-extracellular matrix adhesion and also serve as one of the families of adhesion molecules active in cell-cell adhesion (40). Currently, 24 different functional integrins have been identified and have been determined to bind extracellular matrix proteins and mediate cell-extracellular matrix interactions (40, 41). Extracellular ligands have been found to

include: fibronectin, fibrin(ogen), laminin, various collagens, entactin, tenascin, thrombospondin, von Willebrands factor, and vitronectin (40). Extracellular matrix integrin binding has been found to initiate outside-in signaling, alter gene expression and effect cell survival, proliferation and differentiation (41). Mechanistically, integrin adhesion receptors link the extracellular matrix to cytoskeletal actin and transmit biochemical force across the plasma membrane (41). Cytoskeletal linkages also enable integrins to regulate cell shape and gene expression, mediating cell adhesion, spreading and migration of the cell on the extracellular matrix (41). As cell migration is essential to proper physiological functioning for regulated movement of cells, including embryonic development, immune responses and tissue maintenance and repair, integrin containing adhesion complexes are necessarily dynamic structures that undergo repeated cycles of formation and disassembly (42). Complex pathways of intracellular signaling regulate integrin assembly and disassembly, requiring an intact and physiologically functioning cell to regulate detachment (42).

Lack of these integrin dependant survival signals during cell detachment results in a form of apoptosis known as anoikis, a Greek term meaning homelessness (41, 43). Specifically, the  $\alpha 5 \beta 1$  integrin receptor is known as the fibronectin binding receptor and has been found to be highly expressed in quiescent endothelial cells (43-45).  $\alpha 5 \beta 1$  has also been found in cell-cell contacts and to mediate survival signals despite the loss of cell-matrix anchorage (45).

As endothelial cell detachment is a limiting factor in vascular and corneal preservation, the assessment of cellular adhesion was central to the scope of this work, therefore it became essential to quantitatively measure cellular adhesion following freezing. Previously developed assays such as ECIS, QCM and OWLS use electrical resistance, adsorbed mass and viscoelastic measurements and refractive index respectively to provide information regarding cell-substrate interactions, cell-cell contact and strength of the cell adhesion (46). While these methods are useful indicators for cellular adhesion and confluence the mechanism of assessment limits the ability to measure monolayer adhesion directly post-thaw. In addition, these methods do not indicate if the whole cell or cell remnants are remaining attached to the surface. A

method which concurrently quantifies cellular adhesion and viability was preferentially selected for experimental analysis.

### **Experimental Motivation**

Several studies throughout the literature have examined the effects of cryopreservation on single cells, monolayers, corneal and vascular tissue. A study by Lehle et al. investigated the response of HUVEC suspensions exposed to 10% DMSO in a high-potassium solution followed by cooling at 1 °C/min to -80 °C and storage in liquid nitrogen (36). Their results indicated cryopreservation resulted in a retrieval of 66 +/- 5% and viability of 79 +/- 3% post-thaw (36). While monolayers are known to be less successfully cryopreserved, studies have examined several different cell types of monolayers and have reported various ranges of post-thaw recovery. In one study Pegg used an immortalized human endothelial cell line either as single cells or as confluent monolayers on microcarrier beads and exposed them to 10% DMSO (29). Using various cooling rates down to -180 °C, this study found maximal survival (45-50%) with cooling rates between 0.3 and 10 °C/min (29). While both these studies investigated the response of HUVEC to low temperature exposure in the presence of DMSO, the study by Lehle did not examine the effects of adhesion on HUVEC preservation. Similarly, while the study by Pegg did examine the role of cooling rate variability on adherent monolayers and HUVEC suspensions, the study did not examine the loss of cellular adhesion as a result of low temperature exposure.

A study by Ebertz and McGann used human corneal endothelial cell lines to produce endothelial monolayers and exposed them to 2, 4 or 8 M DMSO (3). A graded freezing protocol was used to cool cells at 1 °C/min to various subzero temperatures to -40 °C followed by direct thaw or cooling to -196 °C or -80 °C for storage, followed by thawing (3). SYTO and ethidium bromide (EB) staining were used as a viability indicators and image analysis software was used to quantify viability (3). However, while cellular detachment was noted in this study, a qualitative grading scale was used to assess the level of detachment in each sample image, indicating adhesion analysis was subjective and more quantitative adhesion assessments should be performed (3).

Previous studies on hypertonic exposure in cell monolayers have used V79 Chinese hamster cell lines and exposed them to concentrated NaCl solutions up to six

times isotonic (47, 48). The study by Hetzel et al. found in unfrozen experiments that attached cells survived exposure to hypertonic environments better than cell suspensions and attributed this finding to a reduced cation flux as a function of a reduced exposed membrane surface area in adherent cells (47). However, in freezing experiments it was found that when exposed to -196 °C, cell suspensions had increased survival (47). While this study investigated the effects of hypertonic exposure in both freezing and non-freezing conditions the high solute concentrations used could itself be damaging to the cells. Also the methods used to obtain adherent cells used trypsinized confluent monolayers which were re-plated and allowed to incubate for 2 hours likely not allowing cells time to re-establish intercellular connections and communication. As this study used an animal cell line known to lack gap junctions, investigation of a human endothelial cell monolayer exposure to freezing conditions will contribute to the knowledge of intercellular adhesion response necessary for the physiological functioning of endothelial cell layers.

### **Objectives of the Thesis**

Human Umbilical Vein Endothelial Cells (HUVEC) were selected for this study. Endothelium *in vivo* is one of few cell types which is a single cell layer thick (49). Therefore confluent HUVEC cultures represent some aspects of the *in vivo* system and as a result were chosen to study the response to freezing in a confluent monolayer.

The purpose of this work was to identify some of the effects and the response of the monolayer in a freezing environment. Studies have indicated endothelial cells become detached during the cryopreservation process. Viability and adhesion are distinctly different; preservation may significantly affect adhesion but not viability or *visa versa*. An investigation of viability will indicate if freezing is damaging to cellular integrity. Conversely, examining cellular adhesion following freezing will provide an indication if cell-surface adhesion is destroyed. It was therefore hypothesized that freeze induced stress to adherent HUVEC monolayers affects viability and attachment differently and may be modulated independently to create new strategies for cryopreservation. The specific objectives were to: to develop a method of quantitatively detecting confluence in the HUVEC monolayer; to develop appropriate methods of

analyzing attachment and viability in monolayers; to define the conditions under which HUVEC undergo detachment as a result of freezing; to define conditions under which HUVEC maintain viability as a result of freezing; to determine the cellular adhesion and viability in a monolayer in response to osmotic exposure prior to preservation.

## **Chapter 2 – Assessment Techniques for Cell Monolayers**

### **Introduction**

With any experimental system, the importance of developing reliable, repeatable and accurate assessment tools is critical for the development of well established experiments and proper interpretation of results. As a means of establishing confidence in the cell analysis tools used to assess viability and adhesion, it was necessary to justify the viability indicator stain SYTO/EB, and to validate the image capturing and the image analysis software Viability 3. With confidence in these experimental systems, accurate assessment of viability and adhesion in Human Umbilical Vein Endothelial Cell (HUVEC) monolayers could be performed.

Experimental methods were developed to assess cellular viability and adhesion using adherent HUVEC attached to cell culture coated coverslips and subsequently exposed to various cryopreservation conditions. In order to measure viability a dual fluorescent membrane integrity stain, SYTO 13 and Ethidium Bromide (EB), was selected to indicate live and dead cells respectively, as well as cellular adhesion. As a cell nucleic acid fluorescent stain, SYTO is able to permeate cells and stain nuclear DNA with UV-excited green emissions (3, 50). EB enters only cells with damaged plasma membranes and forms a red complex with nuclear DNA (3, 50). Commonly used throughout the literature, SYTO/EB staining is described as an effective measure of viability in cryobiology as the plasma membrane is the most likely target of cell injury (18, 50).

SYTO 13 was specifically selected as it has been found to have superior membrane permeability and fluorescence enhancement characteristics when compared to other viability indicators such as fluorescein diacetate (FDA) and 3-(4,5-dimethylthiazol-2yl)-2,5-diphenyl tetrazolium bromide (MTT) (50). SYTO has a slower rate of photo-bleaching than FDA, therefore allowing for longer visualization of the samples (50). SYTO was also found to localize to individual cells in the sample, allowing determination of viability in individual cells and detection of viability patterns and

adhesion, as opposed to MTT or FDA which only provide an overall assessment of the sample and are unable to discern individual cells (50).

Many studies have shown that endothelial cells detach as sheets from the underlying extracellular matrix following cryopreservation (3, 31, 32, 34, 36, 39). Quality image capture of experimental samples after experimental treatment is necessary to observe and analyze patterns of cell adhesion in response to experimental exposure. Colorimetric analysis software was created by Dr. Locksley McGann to identify and count individual cells and determine, from fluorescent SYTO/EB stain, live versus dead cells. Use of computerized image analysis allowed more reproducible data and eliminated variability produced from manual image analysis. However, as the analysis software is based on the principles of colorimetry, accurate and consistent image capturing was required. Image analysis became inconsistent if contrast, white balance or other features were improperly set on the image capturing equipment. Overexposure of images also led to inconsistent data as bright green pixels shifted towards yellow and overlapped with the assessment of red pixels used to identify dead cells, resulting in misrepresentation of live cells as dead. As accurate experimental representation is fundamental to the relevance of scientific findings, the objective of this chapter is to describe and justify the assessment tools used to analyze cellular viability and adhesion in a HUVEC monolayer.

### **SYTO/EB Cell Staining**

In order to assess the ability to quantitate SYTO/EB staining in HUVEC monolayers, HUVECs were grown on fibronectin coated coverslips as described in Chapter 3. The dual fluorescent staining solution SYTO/EB was composed of a final concentration of 0.5 mM SYTO (Molecular Probes) and 0.25 mM EB (Sigma) in isotonic phosphate buffered saline (PBS) (Stem Cell Technologies).

Cell monolayers on coated coverslips were placed in 20 mL scintillation vials and covered with 1.5 mL of fresh EBM-2 (Clonetics) cell culture media. Cells were stained for viability by first warming the cells within the vials to 37 °C in a water bath for 5 min. 150  $\mu$ L of SYTO/EB staining solution was then added to the 1.5 mL of cell culture media and allowed to incubate for 5 minutes at room temperature with the cells. Monolayer

coated coverslips were then gently removed from the glass vial with forceps and inverted on 10  $\mu$ L of cell media with SYTO/EB stain on a glass slide. Cells were then examined under a Leitz microscope at 100x magnification. Five images per monolayer sample taken sequentially across the width of the coverslip were collected with Pax it! imaging software.

Figure 1 shows images of viability staining with dual fluorescent stain SYTO/EB where red cells indicate cells with compromised cell membranes and are considered dead. Green cells are an indication of cells with intact cellular membranes, indicating live cells. This staining technique also provides a means of evaluating cell adhesion as large black spaces indicate areas where cells have detached. Captured images of SYTO/EB stained cells provide representations of live versus dead after cryoinjury and allow visualization of patterns of cell loss. While SYTO/EB provides a reliable measure of viability it indicates the upper limit of cell recovery since there is no indication if the cells are damaged internally or are in the early stages of apoptosis (51).

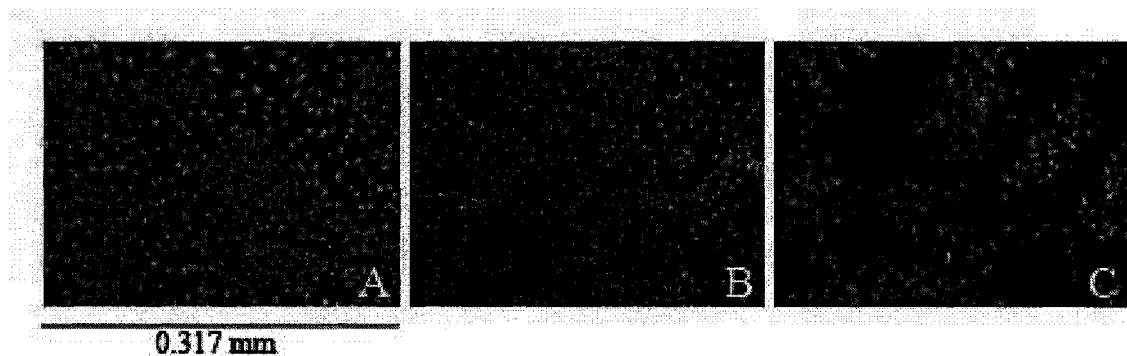


Figure 1. Examples of fluorescent nuclei in cells stained with SYTO/EB showing live green cells (A), dead (red) cells (B) and patterns of detachment indicated by black areas between green and red cells (C).

### **Quality Image Capture**

In an effort to ensure images accurately captured colors in SYTO/EB stained samples, optimization of camera settings was performed. Inappropriate camera settings leading to overexposure of cell samples cause bright green regions to appear yellow (Figure 2). As the computer color capture system uses red-green-blue color identification parameters, overexposure results in red appearing in bright green regions of the image,

therefore appearing as yellow. Yellow within these images is interpreted as red (dead) cells by the imaging software, falsely reporting the image viability.

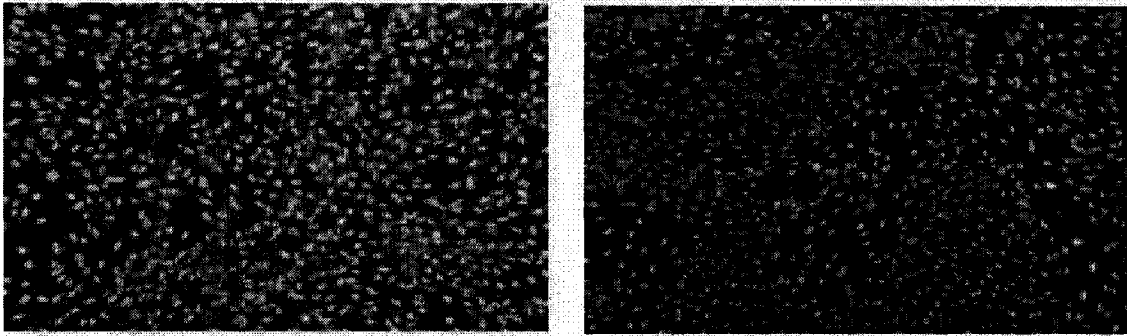


Figure 2. Representative images of overexposed (left) and properly exposed (right) images, indicating the yellow color distribution in the overexposed image.

Departmental photographer, Tom Turner, was consulted and assisted in ensuring proper camera adjustment and color calibration (52). Auto white balance and post image processing features were turned off and all other settings were adjusted to the default setting established within the image capture software. The settings were not subsequently adjusted again thereafter and all experimental images were captured with the identical settings. It was also ensured the fluorescent microscope bulb was turned on 15 minutes prior to experiments and amount of bulb usage was also tracked to ensure the bulb was working efficiently and did not affect sample intensity.

### **Image Analysis Software**

The cell analysis program, Viability 3 (Program interface is pictured in Figure 3), written by Locksley McGann and used herein without alteration, provides cell image analysis including:

- Total number of cells
- Total number of red cells
- Total number of green cells
- Total number of red pixels
- Total number of green pixels
- Percent green cells
- Percent green pixels

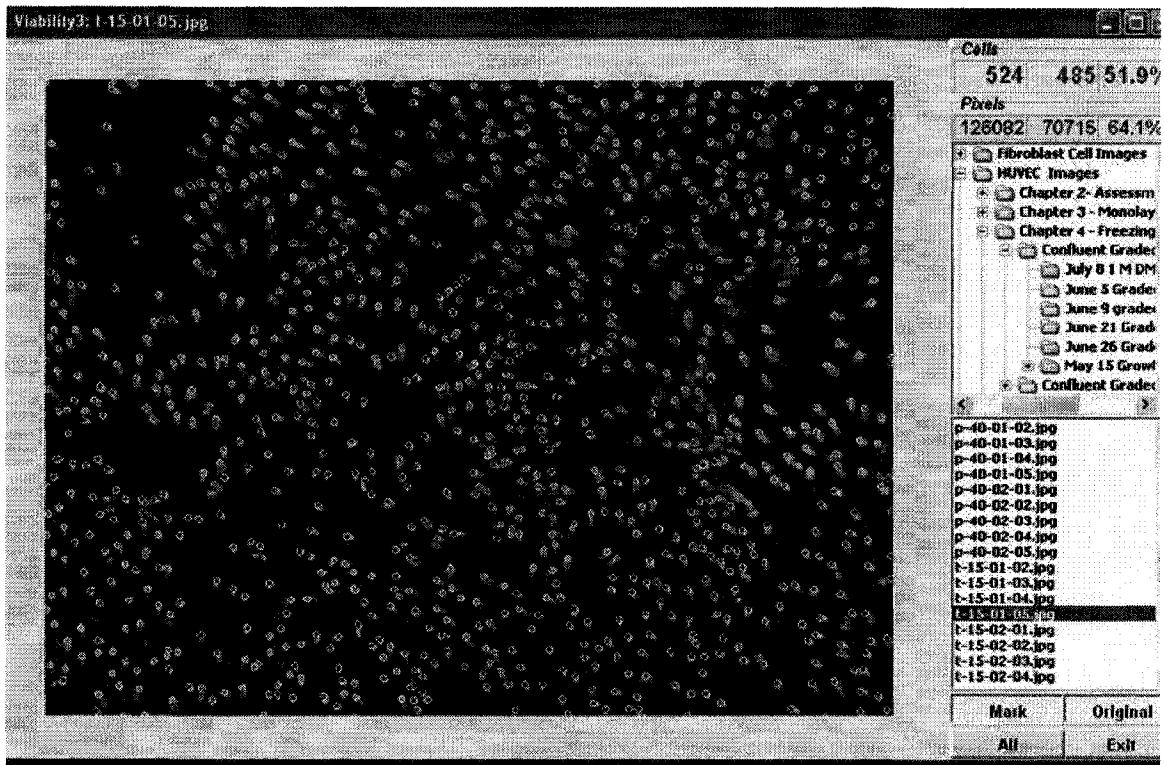


Figure 3. Interface of Viability 3 program. Green and red dots over cell nuclei indicate cell has been counted in analysis and indicate determination of live or dead. Marking of individual cells provides visual confirmation of accurate program cell count.

While the program provides a percent viability for each image calculated as:

$$\text{Relative viability (\%)} = \frac{\text{Number of green cells}}{\text{Number of red + green cells}} \times 100$$

the value produced represents the relative viability and does not account for the cells lost in treatment. Assumptions were made regarding uniform cell seeding, near 100% viability in control samples and near 100% adhesion of control samples were made so that absolute viability could be determined. Absolute viability was a more accurate representation of cell viability calculated as:

$$\text{Absolute viability (\%)} = \frac{\text{Number of green cells}}{\text{Number of green cells in control image}} \times 100$$

Figure 4 demonstrates the distinction between relative and absolute viability using experimental images.

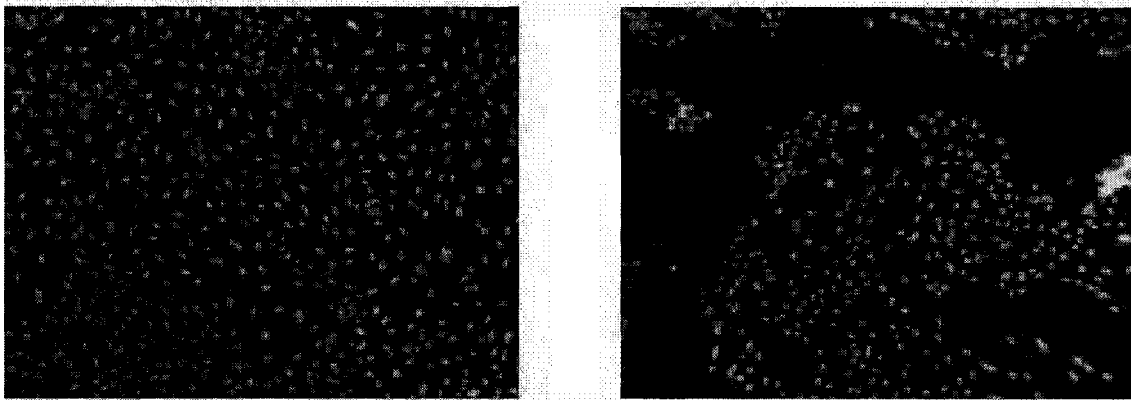


Figure 4. Representation of absolute versus relative viability. Control image is presented on the left and the experimental image on the right. The image on the right has a relative viability of 72.4%. When calculated relative to the control on the left there is an absolute viability of 56.3%.

Similarly, percent absolute adhesion was calculated as:

$$\text{Absolute adhesion (\%)} = \frac{\text{total number of cells in each image}}{\text{total number of cells in control images}} \times 100$$

All results are reported as absolute cell adhesion and absolute cell viability unless otherwise indicated.

### **Manual Justification of Cell Counting Software**

Versions of this viability program have been used in several other studies to assess viability including with articular cartilage, V79-W Chinese hamster fibroblasts, Madin-Darby canine kidney (MDCK) cells, and Human Corneal Endothelial Cell (HCEC) monolayers (3, 28, 51, 53-55). Validation of a previous version has been performed by Johma et al. who determined the program was useful for image analysis of cell viability (51). Johma et al. compared computer analyzed articular cartilage images with images manually counted by experienced, novice and unskilled human counters (51). Their evaluation determined that manual counting can vary within and between evaluators, studies and labs, and identified problems such as perception, color blindness and amount of time consumed as factors which increase the possibility of human error (51).

As a means of justifying the use of the Viability 3 program for the HUVEC cell model and experimental conditions used for this work, manual cell counting by the same

assessor was performed for 10 images, selected from a pool of experimental images representative of the range of experimental results, and compared to data produced from Viability 3 for the same images. Using experienced evaluator manual counting as the gold standard of measure, it was determined there was a difference of  $5.53 \pm 1.41\%$  in cell count and  $5.48 \pm 1.78\%$  in absolute viability between manual counting and Viability 3. Manual counting of cells tended to produce cell counts higher than the viability program, likely due to the software which counts cells in contact as one cell. Viability assessment was also higher in manual counting versus the viability program as cells which appear yellow are counted by the software as dead. Although there is a 5.5% difference in assessment between the manual and Viability 3 counts, we determined it is acceptable to use Viability 3 for assessments in this study because the same algorithms applied to all samples, it conservatively underestimates cell viability and it eliminates counting errors introduced by human variability.

#### **Qualitative Justification of Cell Density as an Indicator of Adhesion**

Cell adhesion was defined by this author as cellular attachment to a cell culture treated surface, which for experimental purposes was a coated glass slide. Previously reported in the literature, the loss of adhesion is normally qualitatively assessed using a subjective visual grading scale (3). However it was thought a more precise quantitative method of assessing adhesion was required; therefore a more objective assessment technique was investigated. To compare and ensure the accuracy of our objective assessment a qualitative adhesion grading scale based on visual assessment was developed (Figure 5), assigning grades from 1 (for the greatest degree of detachment) to 5 (for minimal detachment). Fifteen images were selected from the experimental image pool and manually assessed with a grade according to the grading scale. The same images were then analyzed with Viability 3, where adhesion was calculated as the percentage of cells in the experimental samples compared with untreated controls. Figure 6 shows the correlation between the qualitatively assigned adhesion assessment and quantitative assessment with Viability 3.

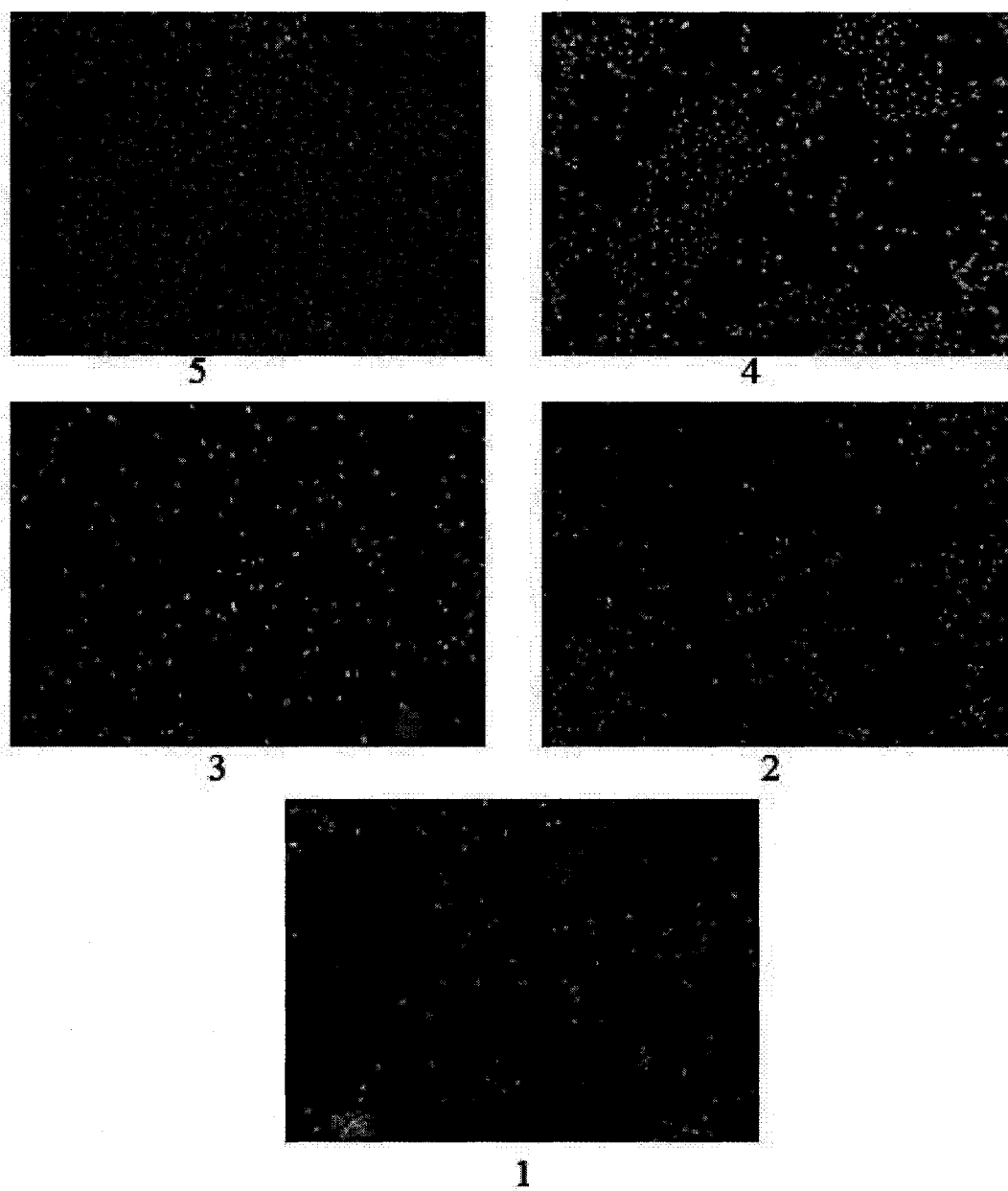


Figure 5. Cell adhesion grading scheme. Cell density is greatest at 5 and decreases to the lowest cell density, designated as 1.

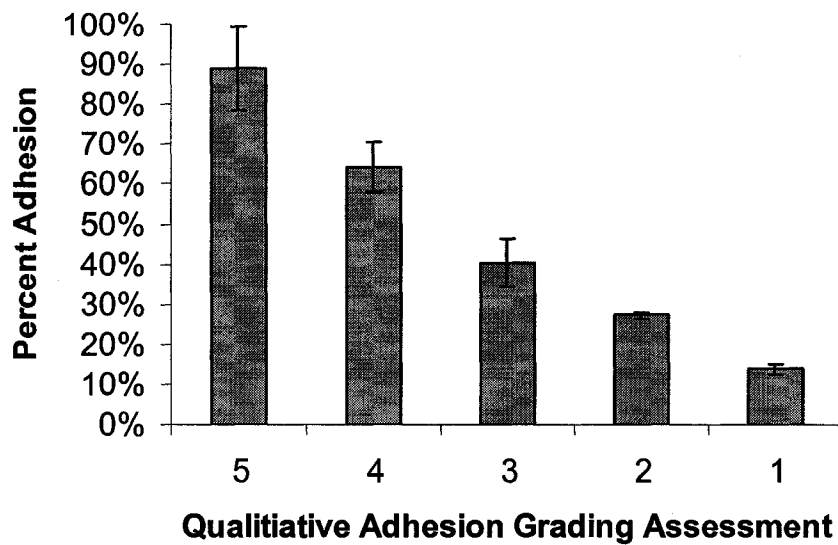


Figure 6. Assessment of adhesion comparing the quantitatively determined cell density using Viability 3, to the qualitatively assigned adhesion grading.

The  $R^2$  correlation coefficient between assessments using the Viability program and the manual adhesion grading scheme was 0.9764. Based on the high correlation between manual and quantitative assessment it was determined that the Viability program was appropriate for use as an alternative to manual adhesion grading.

While in most cases there was an evenly distributed loss of adhesion in experimental samples, patterns of cell detachment, referred to by the author as patchiness, were also observed under certain experimental conditions. For the purpose of this study, patchiness was defined as the loss of cells in sheets, leaving areas of cell clumps surrounded by areas without cells. As our classification of patchiness was unique to this study and no previous analysis methods had been determined in the literature, subjective assessments of patchiness were used. The difference between patchiness and loss of adhesion is illustrated in Figure 7. References to patchy cell loss will be described throughout.

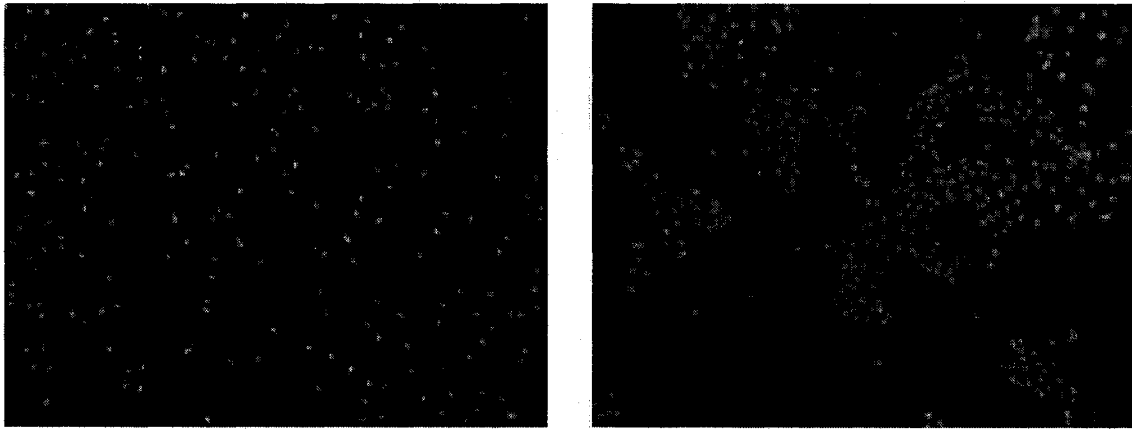


Figure 7. Loss of adhesion and patchiness. The image on the left shows evenly distributed cell loss; however the image on the right shows cell loss described as patchy

### **Discussion**

Accurate assessment techniques to determine viability and adhesion are central to the scope of this work. The SYTO/EB dual fluorescent membrane integrity stain, widely used to assess cryoinjury, was used as a viability indicator for HUVEC monolayers. Use of this technique allowed concurrent measures of viability and cell adhesion as only the nuclei of each cell are stained, giving distinct visualization of each cell present on the coverslip. This method is preferable to other techniques such as MTT and FDA which stain the cellular cytoplasm, as a result staining the cell mass as a whole, eliminating the ability to identify individual cells. Camera settings were also optimized to adjust for overexposure, image processing and white balance. Once the optimal camera settings were determined, all experimental images were taken with these settings.

The Viability 3 cell image analysis software was shown to be effective for determination of absolute counts of live and dead cells, which allows calculation of absolute cell viability. The use of absolute cell viability allows more accurate representation of cell recovery by taking into account cells lost during the experimental procedure.

While a minor error margin between manual and automated image analysis was discovered, use of computer analysis eliminates human error and marginal error produced was found to under-estimate absolute cell viability by 5.5%, indicating data may be counted conservatively. Justification of the program was supported by the findings of Johma et al. (51) and the program has been used in several other experimental protocols

(3, 28, 51, 53-55). An additional benefit was the efficiency of the program which is a remarkable time saving analysis tool as it is estimated that manual image counting would have taken several hundred hours. Qualitative justification was performed by producing an adhesion grading scale which was compared to quantitative data produced by the analysis program for the same images. Results indicated a high correlation ( $R^2= 0.9764$ ) between the grading scale and the quantitatively determined increase in cell adhesion. This correlation demonstrates Viability 3 is appropriate to use as an adhesion assay to assess the number of cells remaining on the coverslip following low temperature exposure.

### **Conclusions**

As a means of ensuring experimental accuracy and efficiency a justification of the chosen experimental techniques was performed. SYTO/EB was selected as a nucleic acid stain since it individually identifies cells and can be used in conjunction with an image analysis program to determine cellular viability and adhesion. Steps were also taken to ensure the microscope camera captured accurate cell images so that viability was not inaccurately determined by the image analysis program. The Viability 3 image analysis program was found to be reasonably accurate when compared to manual cell analysis of both adhesion and viability and was selected for image analysis as it removed human error and significantly lessened the analysis time. As a result of qualitative and quantitative comparisons, techniques were developed to reproducibly assess cell viability and cellular adhesion in monolayers of Human Umbilical Vein Endothelial Cells.

## **Chapter 3 – Optimal HUVEC Growth Curve Conditions and Quantitative**

### **Confluence Analysis**

#### **Introduction**

A HUVEC monolayer was used as the model system. Particular emphasis on developing a well characterized, repeatable cell model system was necessary so that the model could be quantitatively assessed to provide useful information.

Senescent endothelial cells are known to primarily express the  $\alpha 5\beta 1$  integrin fibronectin receptor which recognizes the fibronectin binding proteins expressed in *in-vivo* corneas and vessels (37). Fibronectin protein was chosen to replicate this environment *in-vitro* by coating cell culture surfaces. However, previous research has indicated fibronectin concentration used in cell culture affects cell growth. The substratum has a significant effect on cell morphology, function and gene regulation (56). One study investigated the use of 0, 0.25, 1, 5, 10 and 50  $\mu\text{g/ml}$  fibronectin coating in phosphate buffered saline (PBS) overnight (57). When cell growth was tested on days 2 and 5 after cell plating, cell growth was found to be increased in density with 0.25 and 1  $\mu\text{g/ml}$  (57). That study also determined that vascular endothelial cells respond to high fibronectin concentrations with modest up-regulation of integrin expression, redistribution of integrins and clustering of proteins in focal contacts which assemble in multiple clusters throughout the basal cytoplasm (57). The authors also reported increased actin polymerization and reorganization of the cytoskeleton to couple actin filaments to more numerous adhesion sites, decreased replication and inhibition of growth in the G1 phase which was coincidental with an increased density of cell matrix contacts (57). These findings indicated a need to independently determine the optimal fibronectin concentration for optimal HUVEC growth.

Cell growth occurs in characteristic phases of a growth curve. Figure 1 represents a symbolic cell growth curve as a function of time. Cell growth begins with a characteristic lag phase, as cells recover from storage by freezing or from the trypsinization process to detach adherent cells, resulting in little cell division within this phase. Exponential growth or the log phase follows as new cells are continuously dividing. The cell cycle time for HUVEC is known to be approximately 48 hours (49). Cell replication eventually decreases or stops in the stationary phase. Within this phase

cells become senescent and cell-cell contacts are established. The monolayer becomes confluent when cell-cell contacts are firmly established. As cell growth exceeds the capacity of the culture environment and toxic waste products accumulate and nutrient sources are depleted, cells enter the death phase.

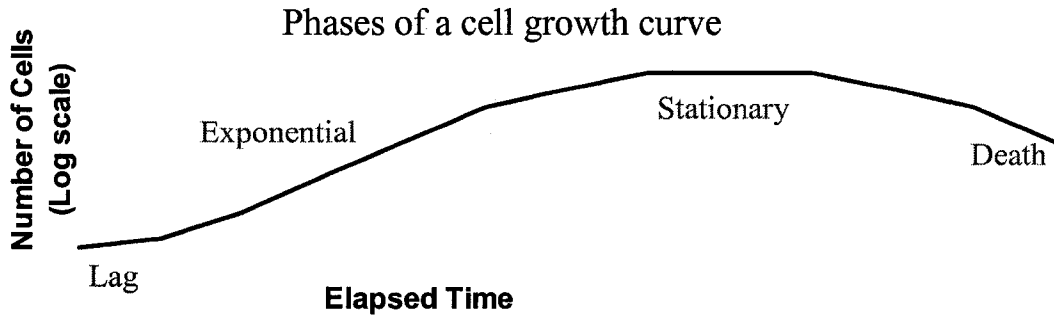


Figure 1. A typical cell growth curve indicating the lag phase, the exponential phase of cell growth, the confluent or stationary phase and the death phase.

### **Determination of Confluence**

Confluence is a common term used in cell culture literature to describe a sheet of cells, growing one-cell-deep on a surface in cell culture. The need to accurately define when confluence has been achieved is essential in this study as cell-cell contact and cell-matrix contact are vital aspects to the study of adhesion. While cell density is not critical, cell-cell contact is (37). Cell-cell contacts themselves, their stability and downstream signals are responsible for regulating mitosis, arresting cells in the G1 phase of DNA replication; prompting confluent monolayers to become senescent (37). Specifically related to the purpose of this study, the development of confluent monolayer models is important to mimic the tight junctions and cell-cell interactions which provide barrier functions and are essential for the proper physiological functioning of vessels and corneas (38). It is also known that cell-cell contacts uniquely affect freeze-thaw responses, therefore the establishment of confluence was important for this study (27).

The limiting factor in consistent assessment of confluence is the lack of available techniques to measure confluence. Currently the most widely used method of evaluating confluence is qualitative experience-based visual observation, where an estimation of the

amount of culture surface area covered by the cells is converted to a percent confluence measure. Recognizing the importance of determining confluence in the study of freezing response of a monolayer, it became evident that, along with the qualitative assessment, a more quantitative confluence assessment was required. The Viability 3 program, described in Chapter 2 was used to determine cell density throughout the growth curve. This method allowed for quantitative values to indicate confluence.

Establishment of a confluent HUVEC monolayer was essential to ensure cell-cell contact and communication within the cell environment was well established. As cell-cell contacts are known to affect the cellular response to cryopreservation it was essential to ensure the monolayers used were well established, confluent, senescent and healthy. The overall objectives were to determine the optimal fibronectin concentration for optimal HUVEC growth, to generate the HUVEC growth curve, and to determine the optimal growth period for producing a confluent monolayer supported by qualitative assessment of cell morphology.

## **Materials and Methods**

### **HUVEC Cell Culture:**

HUVEC cells (Clonetics, Cambrex Bio Science) and were cultured in EBM-2 Bulletkit media (Clonetics), composed of 2% fetal bovine serum (FBS), human epidermal growth factor (hEGF), hydrocortisone, Ga-1000 (Gentamicin, Amphotericin-B), vascular endothelial growth factor (VEGF), human fibroblast growth factor B hFGF-B (with heparin), Insulin-like Growth Factor-I (R<sup>3</sup>-IGF-1), ascorbic acid and heparin. Cell culture media was changed approximately every 48 hours. Cells were cultured in 75 cm<sup>2</sup> tissue culture flasks (VWR) at 37 °C and 5% CO<sub>2</sub> and passaged with a 0.25% Trypsin – EDTA (Gibco) solution when cell density reached approximately 70% of the culture surface. Cells were used at passage 3 for the growth curve experiment.

### Fibronectin Concentration:

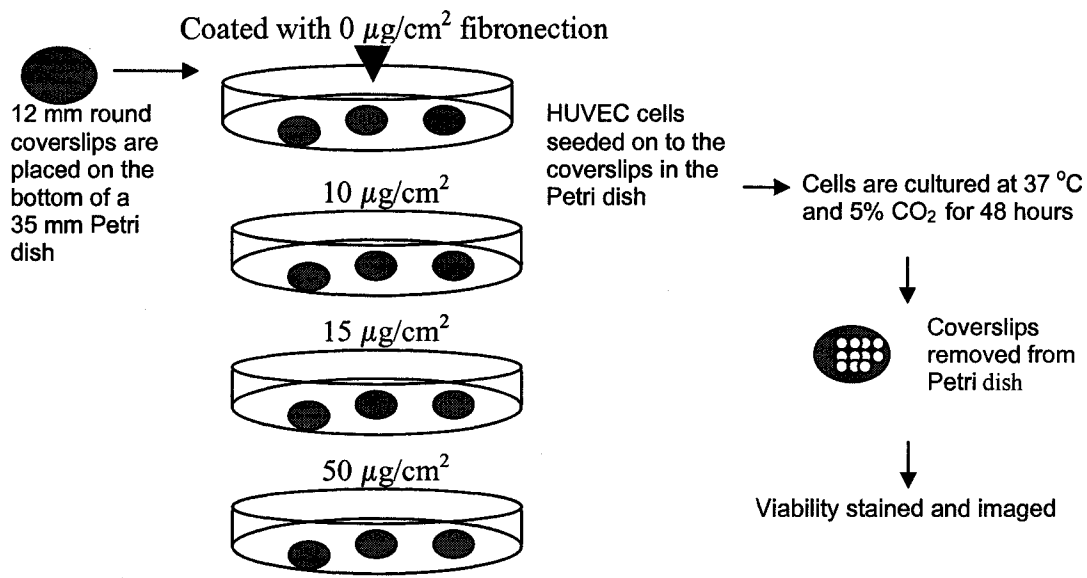


Figure 2. Diagrammatic representation of fibronectin concentration experimental methods.

As shown in Figure 2, 12 mm untreated coverslips (Fisher Scientific) were placed on the bottom of a 35 mm Petri dish (Corning) and coated with 0, 10, 15 or 50  $\mu\text{g}/\text{cm}^2$  human plasma fibronectin (Chemi-Con) dissolved in 1 ml phosphate buffered saline (PBS) (Stem Cell Technologies), containing no  $\text{Ca}^{2+}$  or  $\text{Mg}^{2+}$ , for one hour at room temperature. Unless otherwise stated, all PBS used for fibronectin coating and cell culture was  $\text{Ca}^{2+}$  and  $\text{Mg}^{2+}$  free. The solution was pipetted several times to ensure it covered all coverslips and no coverslips were overlapping. Fibronectin coating solution was removed by aspiration and coverslips washed two times with sterile PBS. A 3% bovine serum albumin (BSA) in PBS blocking solution was then applied to the coverslips to ensure non-specific binding and allowed to incubate at room temperature for 30-60 minutes. After incubation the BSA blocking solution was aspirated off and the coverslips were washed two times with PBS. To ensure the coverslips did not dry out the final PBS wash was aspirated off immediately prior to cell plating.

Once trypsinized from the culture flasks, suspended cells were pipetted several times up and down to ensure all cell clumps were broken up. Counted with a hemocytometer, 600,000 HUVEC cells suspended in 2 mL of the cell solution were added to each dish, ensuring the solution was pipetted evenly across the entire dish to avoid uneven cell plating. Culture dishes were incubated at 37 °C and 5% CO<sub>2</sub> for 48

hours. To determine if pre-coating could be used for experimental convenience three coverslips in a Petri dish, which had been previously coated and stored at 4 °C coated with PBS for 4 days, were cultured in parallel with all other dishes. After incubation, cells were stained with SYTO/EB and imaged as described in Chapter 2. Adhesion was assessed using the Viability 3 software program described in Chapter 2. A total of three coverslips with 5 images per coverslip were assessed for each condition.

Growth Curve:

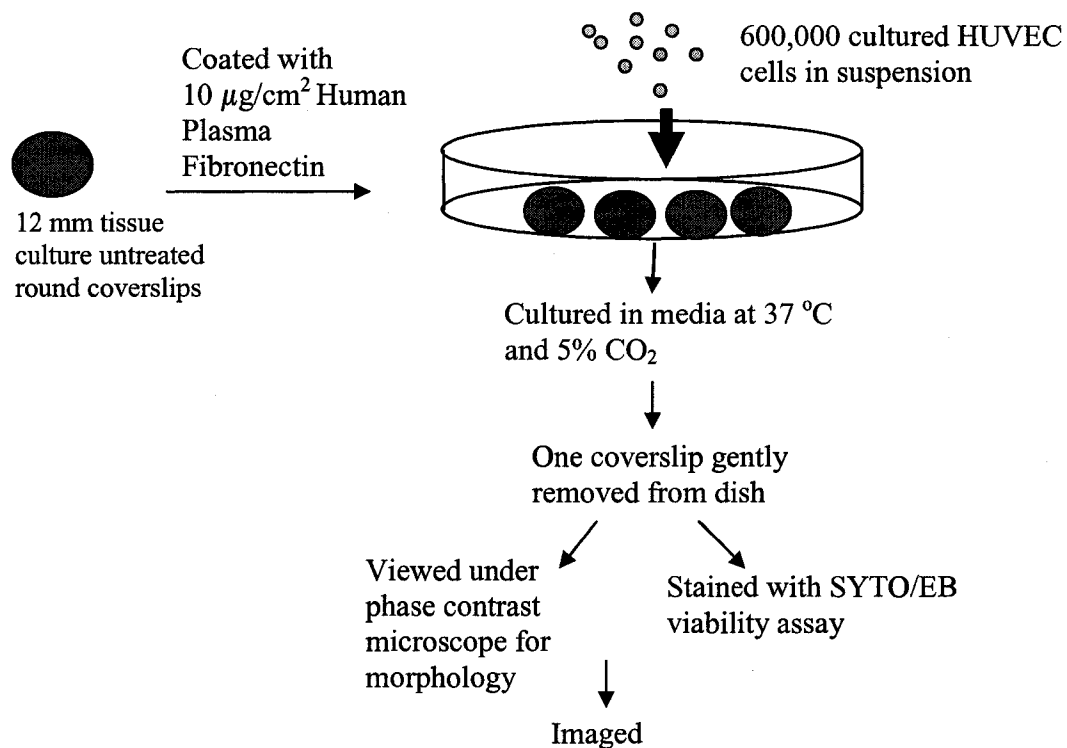


Figure 3. Diagrammatic representation of growth curve experimental methods.

As shown in Figure 3, 4 sterile 12 mm cell culture untreated coverslips (Fisher Scientific) were placed on the bottom of a 35 mm Petri dish (Corning) and coated with 10 µg/cm<sup>2</sup> human plasma fibronectin (Chemicon) and seeded with cells as described above. A total of 15 cell culture dishes were prepared for the growth curve experiment. All growth curve dishes were placed in the incubator at 37 °C and 5% CO<sub>2</sub> and one dish was removed after 3 hours and thereafter each 24 hours after plating.

Growth Curve Analysis:

For each time point sampled, one dish was removed from the incubator. One milliliter of fresh, warmed EBM-2 was added to a new 35 mm Petri dish. One coverslip was gently removed from the original Petri dish with forceps and was placed cell-side up in the new dish. Phase contrast images were captured on an inverted phase contrast Nikon microscope at 100x magnification to provide an assessment of cell morphology. The Petri dish was placed directly on the stage, centering the coverslip under the light source, and 5 images were taken with a Nikon Digital Sight DS-U1 camera. Sequential images were captured as the stage was moved across the width of the dish.

The remaining 3 coverslips in the original cell culture dish were stained with SYTO/EB. Fresh SYTO/EB dual fluorescent membrane integrity stain was prepared, as described in Chapter 2, for each time point. As cells were previously warmed to 37 °C in the incubator, 500  $\mu$ l of cell culture media was removed and 150  $\mu$ L of SYTO/EB stain was added to the original Petri dish and incubated for 5 minutes at room temperature. After the incubation one coverslip was removed from the dish with forceps and placed cell side down on 10  $\mu$ L of SYTO/EB solution on a glass slide. Ten images per coverslip were taken with a Pax Cam and Pax it! imaging software at 100x on a Leitz microscope for each of the 3 coverslips. Cell viability and adhesion were calculated using the Viability 3 cell counting software. In total 3 SYTO/EB stained and 1 phase contrast coverslip were imaged (5 times per coverslip) at each time point to determine the growth curve. An average of the 15 images (5 from each of the 3 SYTO/EB stained replicates) per time point and standard error (estimated standard deviation of the sample mean based on the population mean) were calculated. One experiment was performed.

## **Results**

### **Optimal Fibronectin Concentration**

Figure 4 shows cell density after 48 hours of growth on coverslips coated with various concentrations of fibronectin. Cell growth was highest with 10  $\mu$ g/cm<sup>2</sup> fibronectin concentration. Cell growth was unaffected by coverslip storage for up to 4 days at 4 °C. Cell density was lower in the presence of 0, 15 and 50  $\mu$ g/cm<sup>2</sup> fibronectin.

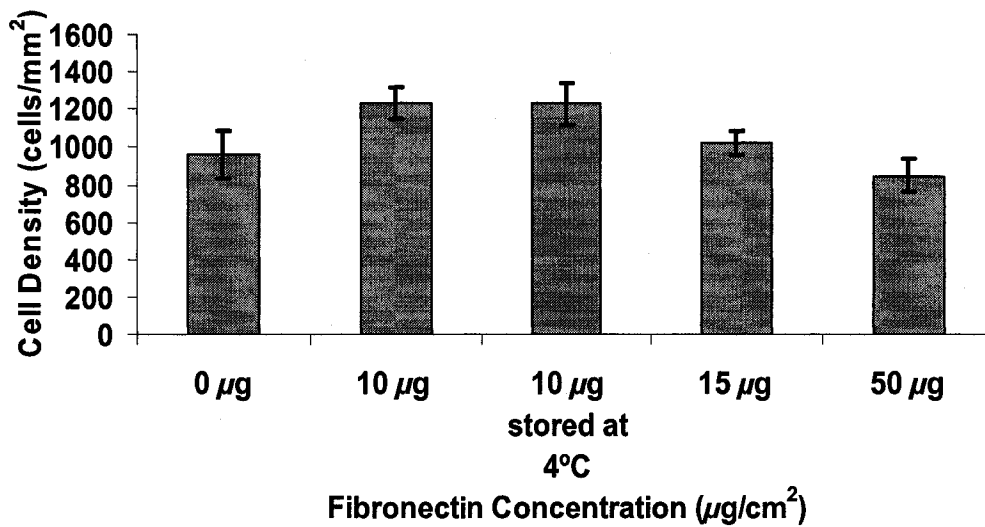


Figure 4. Cell density after 48 h of cell culture as a function of fibronectin coating concentration. Error bars indicate standard error of the sample.

Growth Curve and Quantitative Determination of Confluence

Figure 5 shows the phases of cell growth throughout the growth curve and confirms the stationary phase of growth between days 4 through 9.

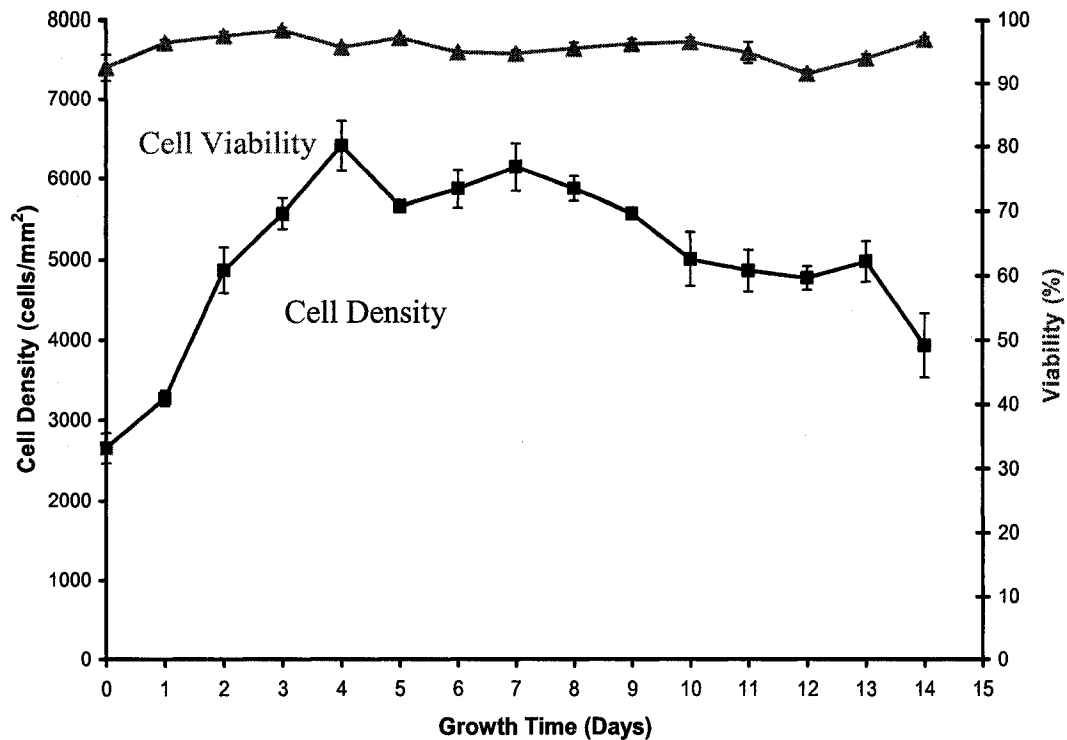


Figure 5. HUVEC growth curve over a 14 day period. Relative cell viability (pink triangles) remains consistent throughout the time period. Cell number (blue squares) follows a characteristic lag phase from day 0 to day 1, logarithmic phase from day 1 to 4, a plateau from days 4 to 9 and a cell death phase from days 10 through 14. Error bars represent standard error of the sample.

Confirmation of confluence was determined by combining quantitative cell density measurements with qualitative assessments of cell morphology. Quantitative assessments were performed on 3 replicates for each 24 hour time point for fluorescent, phase images and cell count analysis. Figure 6 shows a phase contrast representation of cell growth throughout the growth curve. Cell morphology and density were qualitatively analyzed and subjectively determined to be confluent when they exhibited the characteristic cobble-stone morphology (36). Examination of cell morphology in Figure 6 indicated elongated cells prior to day 7, thereafter cells became more evenly rounded and developed the characteristic cobble-stone morphology from days 7 to 9.

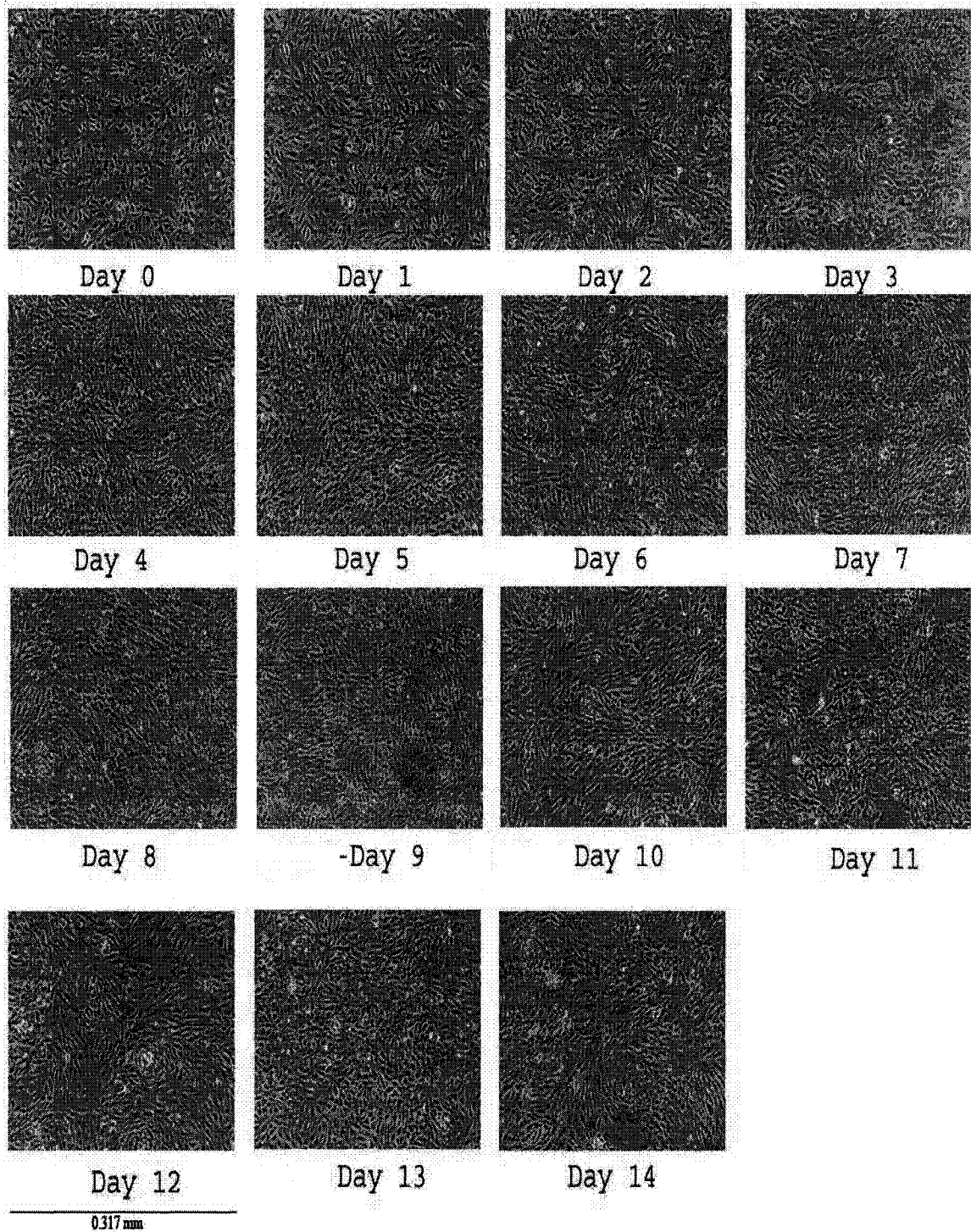


Figure 6. Phase contrast images along the HUVEC growth curve indicating increasing cell density and changes in cell morphology.

Figure 7 shows cell viability throughout the 14 day growth curve and provides an indication of cell density. SYTO/EB stains only the nuclei of individual cells allowing a visual

representation of cell density and cell size consistency as nuclei appear elongated from days 0 to 4 but appear more rounded and evenly sized from days 4 through 9.

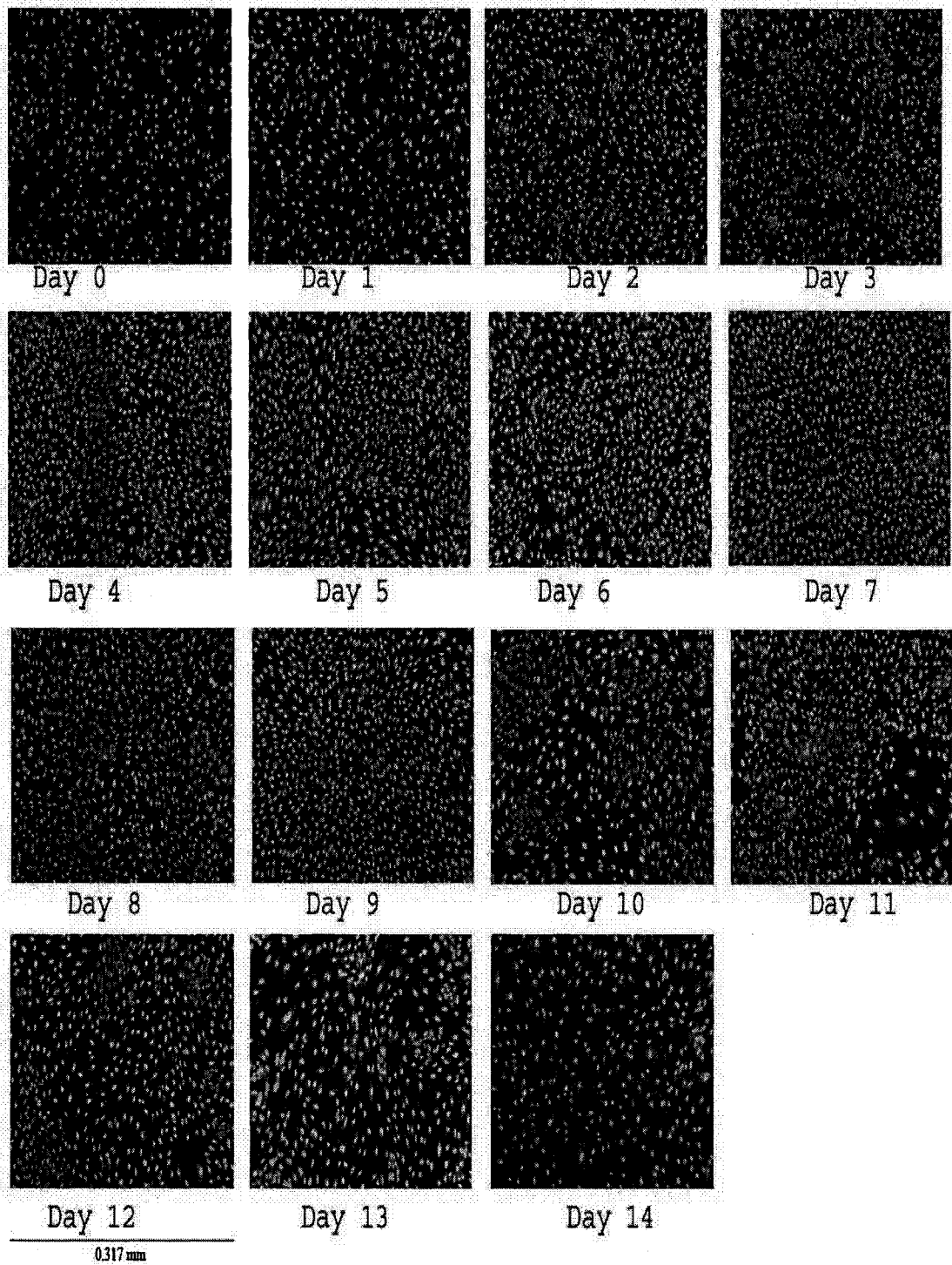


Figure 7. SYTO/EB stained HUVEC growth curve images indicating increasing cell density and relative viability.

Phase contrast and viability images both indicate a plateau of cell growth between days 4 to 9. Image morphology further narrowed the confluence period to between 7 and 9 days. Based on information from these quantitative and qualitative assessments, a 7 to 9 day cell culture preparation was selected to ensure a confluent monolayer for further experiments, as highlighted in Figure 8.

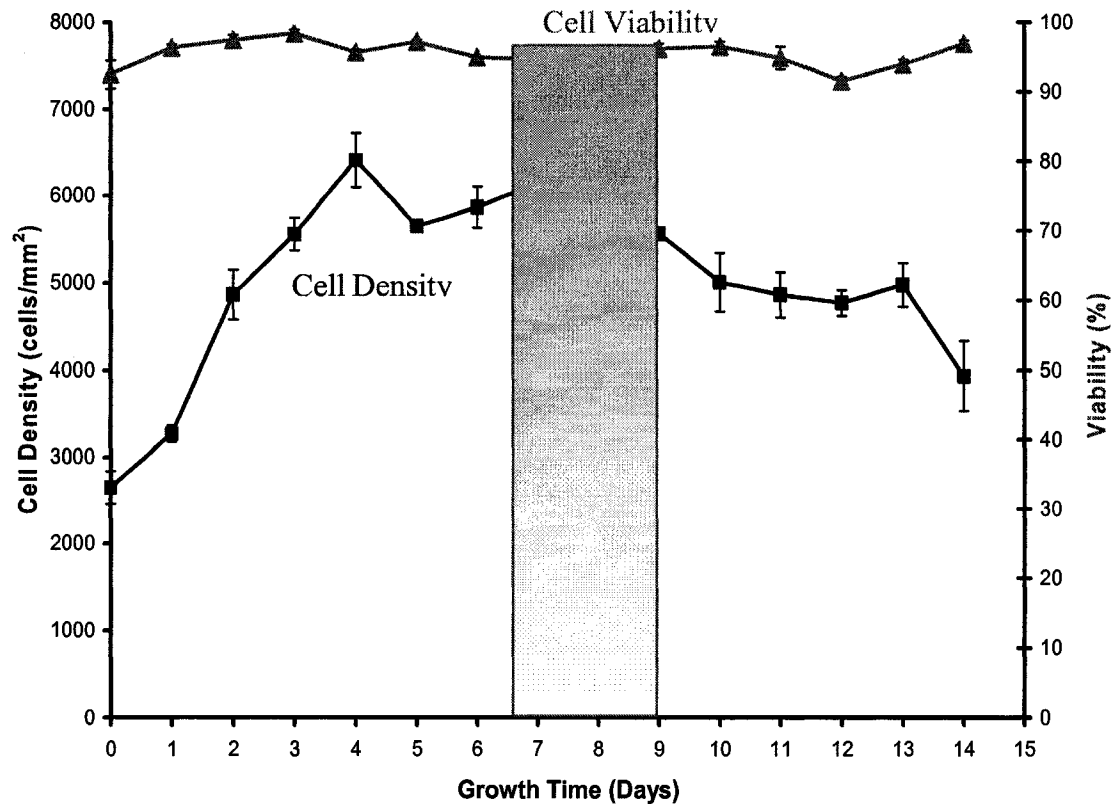


Figure 8. Growth curve highlighting the experimentally determined growth time selected for confluent monolayers to be used in further experiments.

### Discussion

Throughout the literature there are large variations in fibronectin concentrations used in cell culture surface coating with studies reporting 50  $\mu\text{g/ml}$ , 15  $\mu\text{g/ml}$  and 10  $\mu\text{g/ml}$  to be optimal for their cell of interest (58-60). Manufacturer recommended concentrations varied between 2 and 10  $\mu\text{g/cm}^2$ . Due to the variability reported in the literature it was decided to experimentally determine the ideal fibronectin concentration for HUVEC monolayers. Our results correlate with reports of cell growth in the absence

of, and at high concentrations, of fibronectin coating (57). The results showed that 10  $\mu\text{g}/\text{cm}^2$  was the optimal fibronectin concentration, and that pre-preparation and storage at 4 °C of 10  $\mu\text{g}/\text{cm}^2$  coated coverslips did not affect cell growth.

Quantitative analysis of HUVEC growth curves indicated that these cells follow the characteristic growth pattern. The population doubling time in the exponential phase was determined to be approximately 48 hours, consistent with data reported in the literature (49). Using both quantitative cell density and qualitative morphological examination of cell growth, confluence was determined to be between 7 and 9 days of culture. A measure of confluence was essential to ensure consistent production of confluent monolayers. Viability 3 cell counting software was used to accurately determine cell density. Previous justification reported in Chapter 2 indicated Viability 3 is an effective method for measuring cell density. As cells between this period are evenly sized and cobble-stoned in appearance it is likely that cell-cell and cell-surface contacts are well established at this point. Our experimental findings indicated that both quantitative and qualitative assessment technique results were correlated. Determination of cell density in conjunction with an examination of cell morphology improves the confidence in a determination of confluence. As a result both cell morphology (using phase contrast microscopy) and cell density (using SYTO/EB staining and fluorescent imaging) were examined before each experimental procedure.

Post-experimental examination of the literature revealed a study which supported these findings and determined that by one week there is development of single cell thick confluent monolayers of densely packed polygonal cells (49). While there was significant similarity between that study and the results reported here there was a variation of media used to support cell growth as well as the distinction that cell growth did not occur on fibronectin-coated surfaces. Given that our experiment was unbiased by the prior knowledge of the literature result, the correlation between the results supports the strength of our findings. Also in agreement with our findings, a study by Wusteman and Wang used porcine intact corneas and primary cultures of the same cells (61). While the cell type was porcine versus the human cells used in this study, it was nonetheless determined monolayer confluence was achieved within 6 – 7 days (61).

### **Conclusion**

A concentration of  $10 \mu\text{g}/\text{cm}^2$  fibronectin on glass coverslips was optimal for HUVEC and this was unaffected by prior storage of coated coverslips at  $4^\circ\text{C}$  for 4 days. This allows the convenience of pre-coating coverslips prior to experimental use. Data from the growth curve indicated HUVECs grow logarithmically from day 1 to 4, enter a plateau phase until day 9, followed by a death phase. Morphological assessments indicated a cobble-stone morphology, characteristic of a confluent HUVEC monolayer, was achieved between days 7 to 9. Using quantitative morphological assessment supported by cell density, it was decided confluence was achieved between 7 to 9 days. As both the qualitative and quantitative methods of analysis supported and contributed to the findings it is suggested both methods should be used to confidently assess confluence in HUVEC monolayers.

## **Chapter 4 – Cell viability and adhesion after freezing of HUVEC monolayers**

### **Introduction**

A review of the cryopreservation literature indicates many studies have previously investigated the response of cellular monolayers to freezing injury. Limited success of tissue preservation has been achieved; however protection of the unique intercellular and cell-surface interactions is currently lacking in common preservation protocols. Many variations of freezing protocols have been attempted to overcome the limitations of tissue preservation. Limited success has been achieved with classical cryopreservation of corneas and blood vessels, and preservation approaches using vitrification have had difficulties overcoming toxicity from cryoprotectants and devitrification on warming (3, 31). Commonly-used graded freezing protocols use linear cooling to a range of designated subzero temperatures from which samples are directly thawed at 37 °C or plunged in liquid nitrogen at -196 °C followed by removal and re-warming to 37 °C. This graded freezing protocol has been determined to be an excellent technique to differentiate between slow-cool injury (i.e. solution effects damage) and rapid-cool injury (intracellular ice formation) as defined by the two-factor hypothesis of freezing injury (3). Direct thawing after slow-cooling indicates damage due to dilution stress and critical cell shrinkage while thawing after rapid cooling or plunge to -196 °C identifies additional damage by intracellular ice formation (3). Graded freezing protocols have been previously used to measure the effects of slow cool injury in porcine corneas, porcine articular cartilage, V-79W Chinese hamster fibroblasts, MDCK and HCEC monolayers (3, 50, 53). Based on several previous endothelial cell preservation studies a cooling rate of 1 °C/min was chosen (39).

Throughout the cryopreservation literature, DMSO is the cryoprotectant most commonly used for cell preservation. DMSO has been found to be an effective cryoprotectant in monolayers of various cell types. Acker found 10% DMSO increased viability significantly in a freezing protocol at 1 °C/min down to -40 °C followed by a direct thaw at 37 °C in single-attached cells and confluent monolayers for both V-79 Chinese hamster fibroblasts and MDCK cells (62). In the absence of cryoprotectants monolayer preservation yielded approximately a 20% recovery for both cell lines, while the addition of 10% DMSO increased viability in both V-79W and MDCK cells to above

80% (62). Echoing these findings is a study which reported an increase in survival to 70% and 80% of attached vascular endothelial cells stored at -180 °C with the addition of 10% DMSO at low cooling rates of 1 °C/min and 0.3 °C/min, respectively (29). HUVECs were also purchased frozen in suspension in 10% DMSO and high post-thaw recovery was noted (>70%). In light of the reported increase in post-freezing viability, DMSO was chosen for our experimental protocol.

While other studies have used cell monolayer models to investigate cellular response to freezing, no other known published research has developed a method of simultaneous, independent quantification of adhesion and viability. While in Ebertz's thesis investigating human corneal cell response to freezing, quantitative assessment of viability was performed, only preliminary qualitative methods were used to assess adhesion (63). The use of graded freezing, cell staining and analysis techniques will allow the ability to determine if adhesion and viability are independently affected, as well as allow identification of patterns of detachment. Most significantly, the experimental methods presented allow speculations regarding the influence of cell-cell attachments on the cellular response to freezing to be made. The focus of these experiments was to identify and define the freezing conditions responsible for individual HUVEC monolayer response for adhesion and viability. Based on previous monolayer literature, it is hypothesized that HUVEC monolayers will retain approximately 70% viability and adequate adhesion with slow cooling at 1 °C/min in the presence of 1M DMSO. As the maintenance of both cellular viability and adhesion post-preservation are critical to the maintenance of a physiologically functioning tissue, it was decided that conditions responsible for affecting adhesion and viability be identified so that knowledge regarding the response of a HUVEC monolayer to freezing could be increased. The overall objectives of this chapter are to determine the effects of a graded freeze cryopreservation protocol, with and without DMSO, on viability and adhesion in HUVEC monolayer models.

## Materials and Methods

### The Experimental System

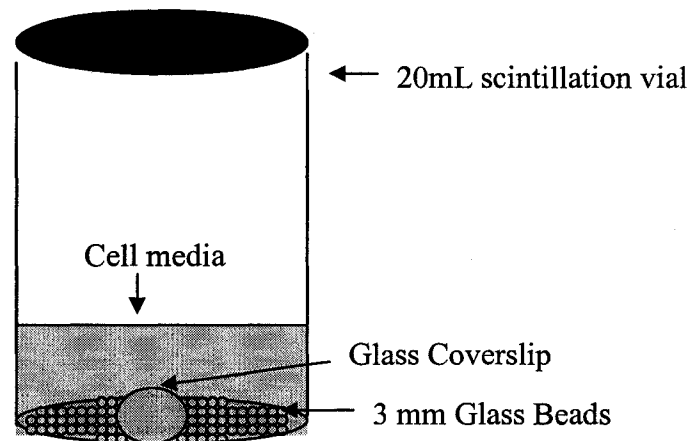


Figure 1. Schematic diagram of the experimental system.

Three millimeter beads (Sigma) lined the bottom of the 20 mL glass scintillation vials (Fisher Scientific) so that coverslips would be raised from the bottom of the vial. The use of beads ensured that coverslips were not in direct contact with the bottom of the vial and could therefore be removed from the vial without disturbing the monolayer. One 12 mm glass coverslip (Fisher Scientific) was carefully added with forceps cell-side-up to each scintillation vial. 1.5 mL of fresh EBM-2 cell culture media was added to each vial ensuring the coverslips were completely submersed. Prior to freezing, all vials were visually inspected to ensure that the coverslip was flat across the beads and not angled, inverted or stuck to the side of the vial.

### Thermal Characteristics of the System

A temperature profile of the experimental set-up (described above) was measured to determine the time required for the experimental system to reach the desired experimental temperature, as well as the hold time after nucleation for the solution to cool back down to a set temperature. Three glass scintillation vials (Fisher Scientific) were lined with 3 mm beads (Sigma) on the bottom surface and filled with 1.5 ml of EBM-2 cell culture media (Clonetics). A type T (Cu-Con) thermocouple (Omega) connected to a data acquisition system (DAQ) was inserted into each vial so that the tip was immersed at the level of the coverslip. Each vial was placed in a methanol bath at  $-5^{\circ}\text{C}$  in a Styrofoam floatation rack to ensure the vials remained upright and adequately

immersed throughout the experiment. The stir mechanism of the methanol bath was adjusted to 85 to ensure even cooling throughout the bath. Temperatures were recorded in 0.15 second increments throughout the course of the experiment. When the vial solution temperature reached  $-5\text{ }^{\circ}\text{C}$  the sample was quickly nucleated with a liquid nitrogen cooled probe. Temperature and time for the sample to initially reach and cool back down to  $-5\text{ }^{\circ}\text{C}$  following nucleation were recorded. The procedure was repeated 3 times.

#### HUVEC Cell Preparation

Four cell-culture-untreated 12 mm round coverslips (Fisher Scientific) were placed flush with the bottom of a 35 mm Petri Dish (Corning) and coated with  $10\text{ }\mu\text{g}/\text{cm}^2$  human plasma Fibronectin (Chemicon) as described in Chapter 3. Each Petri dish was seeded with 600,000 cells suspended in culture media.

HUVEC cells were cultured for 7-9 days in EBM-2 Clonetics cell culture media (Cambrex Bio Sciences) at  $37\text{ }^{\circ}\text{C}$  and 5%  $\text{CO}_2$ . For each experiment, coverslips were gently removed from each dish with forceps and placed cell side up in 20 mL glass scintillation vials with 1.5 mL of fresh, warmed to  $37\text{ }^{\circ}\text{C}$  culture media, either with or without 1M DMSO dissolved in the cell culture media. DMSO, non-DMSO and non-frozen control samples exposed to the experimental solution (0 or 1M DMSO) were equilibrated for 10 minutes at room temperature. Experimental samples were then frozen according to the graded freezing protocol described below. SYTO/EB stain was added to each non-frozen control sample vial and allowed to incubate for 5 minutes at room temperature. Coverslips were then removed from the vial and imaged as previously described.

#### Graded Freezing Protocol

Prior to the commencement of the experiment, the methanol bath was turned on and set to  $-5\text{ }^{\circ}\text{C}$ . An independent type T thermocouple was placed approximately 2 inches from the surface of the methanol and was used in conjunction with a DAQ to measure the bath temperature. Experimental sample vials were positioned in Styrofoam floating racks which were placed in a  $-5\text{ }^{\circ}\text{C}$  methanol bath. According to the results of the prior temperature profile experiment, vials were all held for 3 minutes to allow for cooling to  $-5\text{ }^{\circ}\text{C}$ , then nucleated with a probe cooled in liquid nitrogen. Nucleation of

each vial was performed in a random sequence and all samples were nucleated within an average of 15 seconds. The vials were then held at  $-5\text{ }^{\circ}\text{C}$  for 6 minutes to allow the latent heat of fusion to dissipate. Again the time period of 6 min was based on the results of the prior temperature profile experiment. After 6 minutes at  $-5\text{ }^{\circ}\text{C}$ , 4 vials were removed with 2 being plunged in liquid nitrogen ( $-196\text{ }^{\circ}\text{C}$ ) for a minimum of 20 minutes (plunge condition) and 2 vials being thawed directly (direct thaw condition) in a water bath at  $37\text{ }^{\circ}\text{C}$  for 5 minutes at a warming rate of  $20\text{ }^{\circ}\text{C}/\text{min}$ . The remaining vials were cooled at  $1\text{ }^{\circ}\text{C}/\text{min}$  in the methanol bath and were removed in  $5\text{ }^{\circ}\text{C}$  increments down to  $-40\text{ }^{\circ}\text{C}$  for a plunge and a thaw. Figure 2 shows the schematic representation of the experimental plan. For each temperature condition 4 vials were prepared, 2 for each of each of the plunge and thaw conditions.

## Graded Freezing Protocol Design

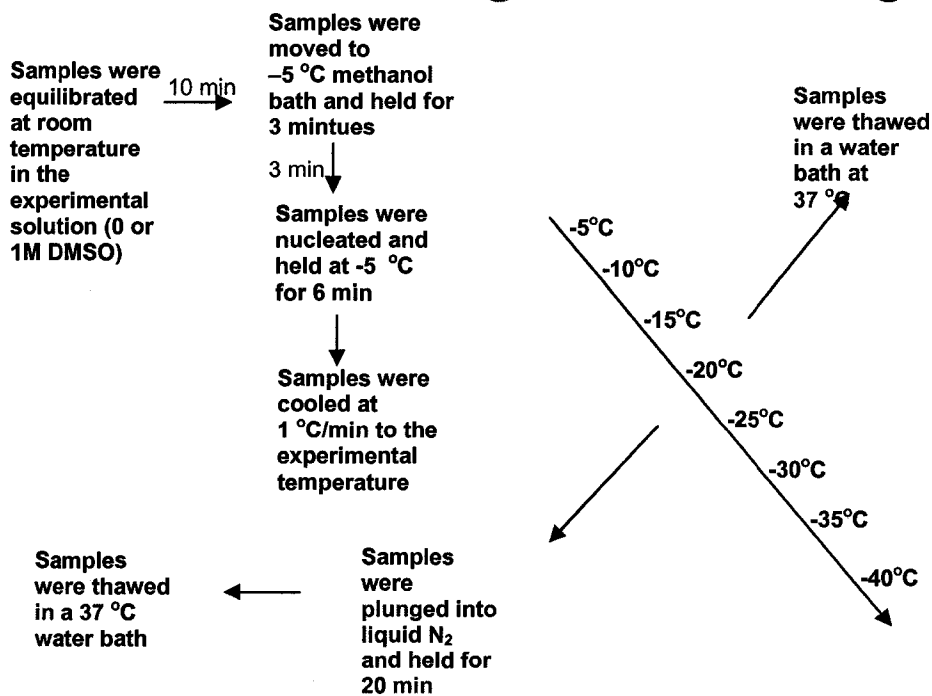


Figure 2. Schematic diagram of the graded freezing protocol.

As the experimental solution was completely frozen at  $-196\text{ }^{\circ}\text{C}$  and the cells were essentially in suspended animation, samples were removed after a minimum of 20

minutes in liquid nitrogen, and thawed directly at 37 °C for 5 minutes. SYTO/EB stain solution (150  $\mu$ L) (described in Chapter 2) was added to each vial, incubating for 5 minutes at room temperature. After incubation, coverslips were removed from the vials with forceps and placed gently cell side down on 10  $\mu$ L of SYTO/EB and media staining solution on a microscope slide. Images were captured on a Leitz fluorescent microscope and analyzed as described in Chapter 2.

## **Results**

### **Thermal Characteristics of the System**

As the samples were cooled, a rapid decrease in temperature was observed down to -5 °C. Figure 3 indicates that the sample reached -5 °C at approximately 2.6 minutes; however Figure 3 represents only a single sample. As the time to reach -5 °C slightly varied between samples it was determined 3 minutes would be sufficient to ensure that all samples have cooled to the bath temperature. Following nucleation a sharp increase in temperature was noted as the sample released its latent heat of fusion. Time was required for the solution to cool back down to the -5 °C bath temperature. As the exact time to cool to the bath temperature again varied slightly between samples, it was determined that 6 minutes is sufficient for the latent heat of fusion to dissipate and ensure all samples have cooled back down to -5 °C.

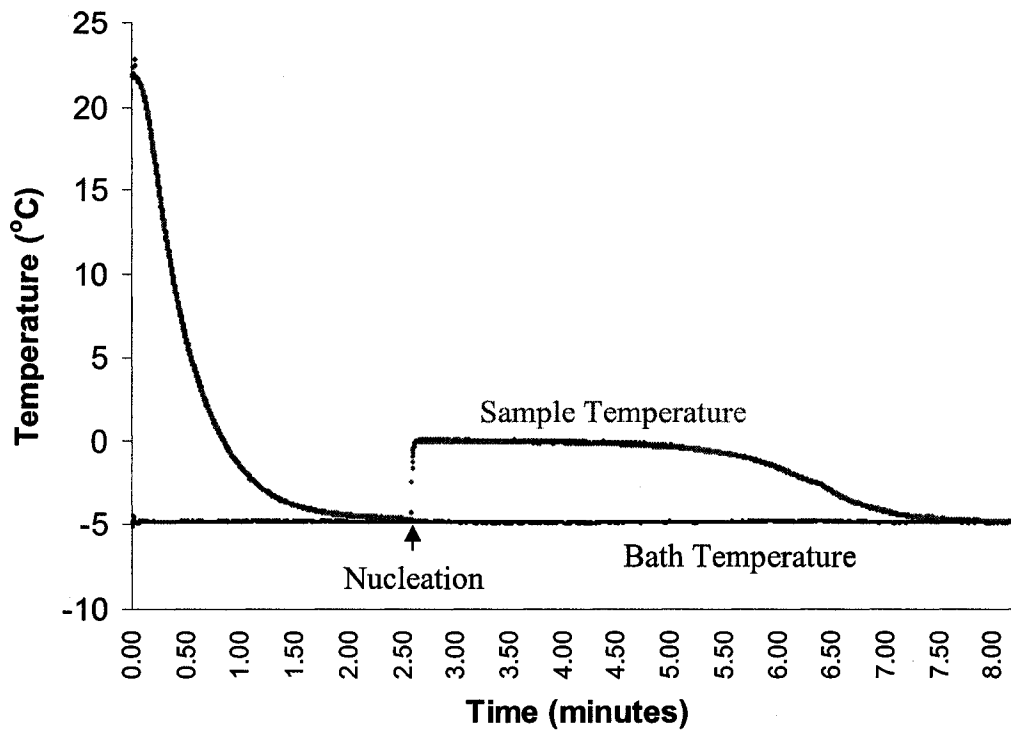


Figure 3. Representative recorded temperature profile with 1.5 mL media in 20 mL scintillation vials placed in a methanol bath at -5 °C.

### Adhesion and Viability of HUVEC Monolayers Following Graded Freezing

Figure 4 shows that adhesion and viability after direct thaw are distinctly affected by exposure to DMSO and a decrease in temperature. The direct thaw condition shows an upward trend in adhesion and a downward trend for viability as the experimental temperature decreases in DMSO and non-DMSO treated samples. DMSO appears to offer little protection for viability or adhesion in directly thawed samples.

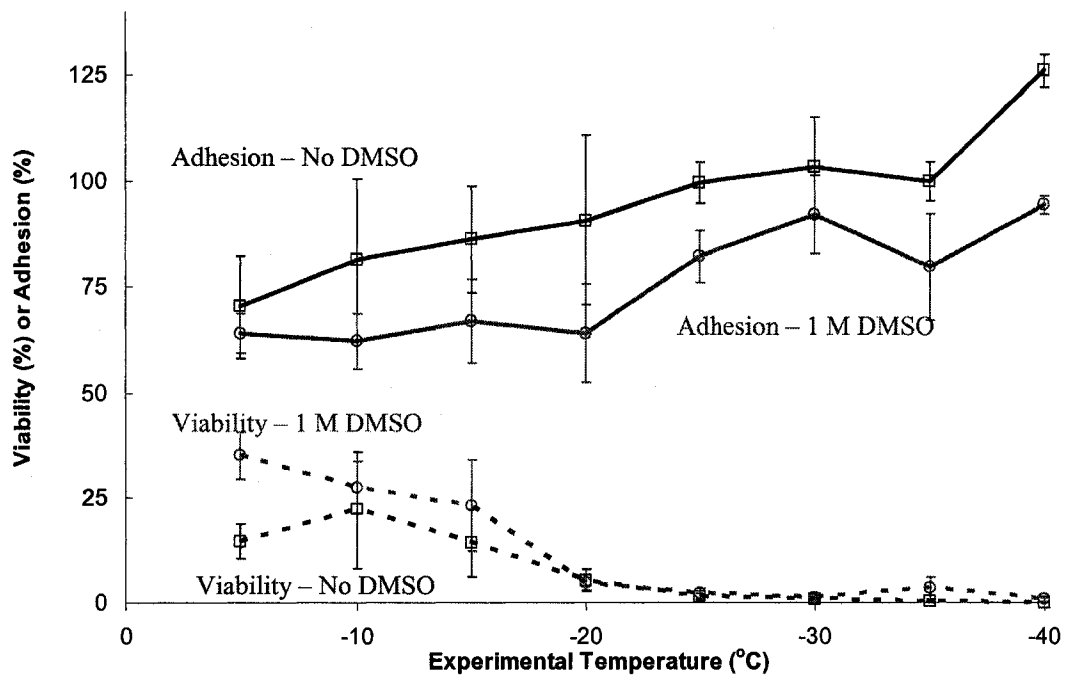


Figure 4. Absolute viability and adhesion for HUVEC monolayers after direct thaw from different experimental temperatures in the graded freezing procedure. The solid lines indicate adhesion and the dotted lines indicate viability. Red indicates samples with 1 M DMSO and blue indicates samples with no DMSO.

Figure 5 shows no noticeable trends when monolayers are plunged to  $-196^{\circ}\text{C}$ , as adhesion remained high throughout the graded freezing protocol. No distinction in adhesion patterns between DMSO or non-DMSO treated samples was noted. The plunge condition resulted in no viability for either the 0 or 1 M DMSO samples from any experimental temperature.

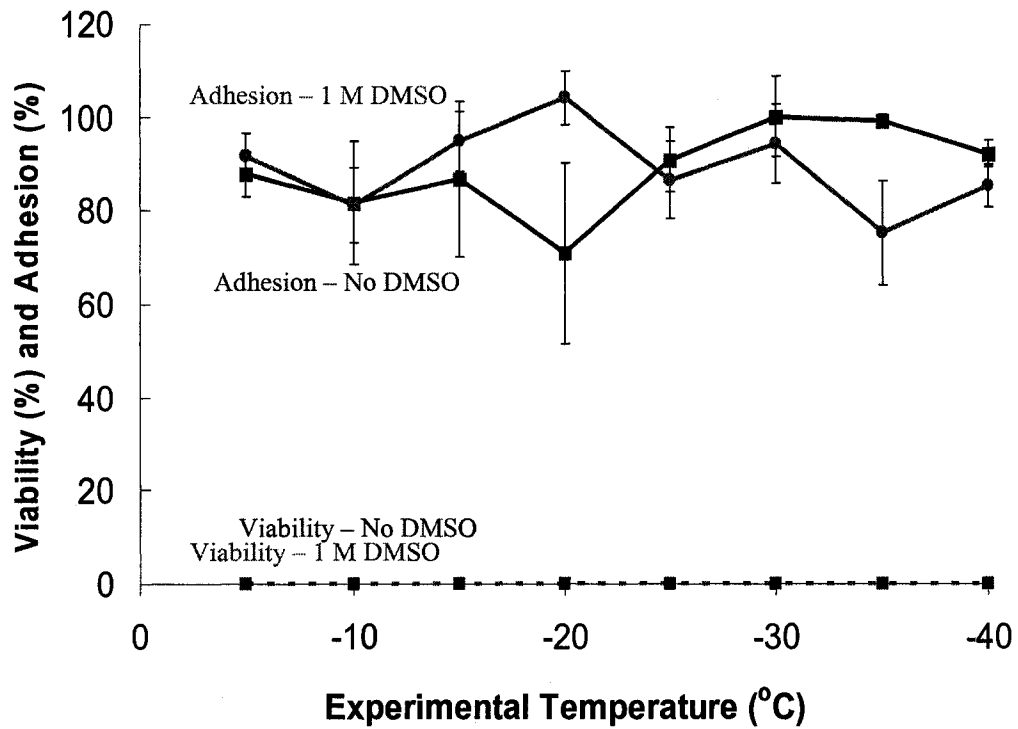


Figure 5. Absolute viability and adhesion for HUVEC monolayers after plunge from different experimental temperatures in the graded freezing procedure. The solid lines indicate adhesion and the dotted lines indicate viability. Red indicates samples with 1 M DMSO and blue indicates samples with no DMSO.

In the presence of 1M DMSO, Figure 6, shows higher adhesion for experimental temperatures above  $-25^{\circ}\text{C}$  in samples plunged to  $-196^{\circ}\text{C}$  compared to samples which were directly thawed from the experimental temperature. For experimental temperatures below  $-25^{\circ}\text{C}$ , there is no difference in adhesion between plunge and direct thaw results for 1 M DMSO. A comparison of viability in plunged and direct thaw samples indicates that cells maintain some viability after direct thaw versus no viability for plunged samples.

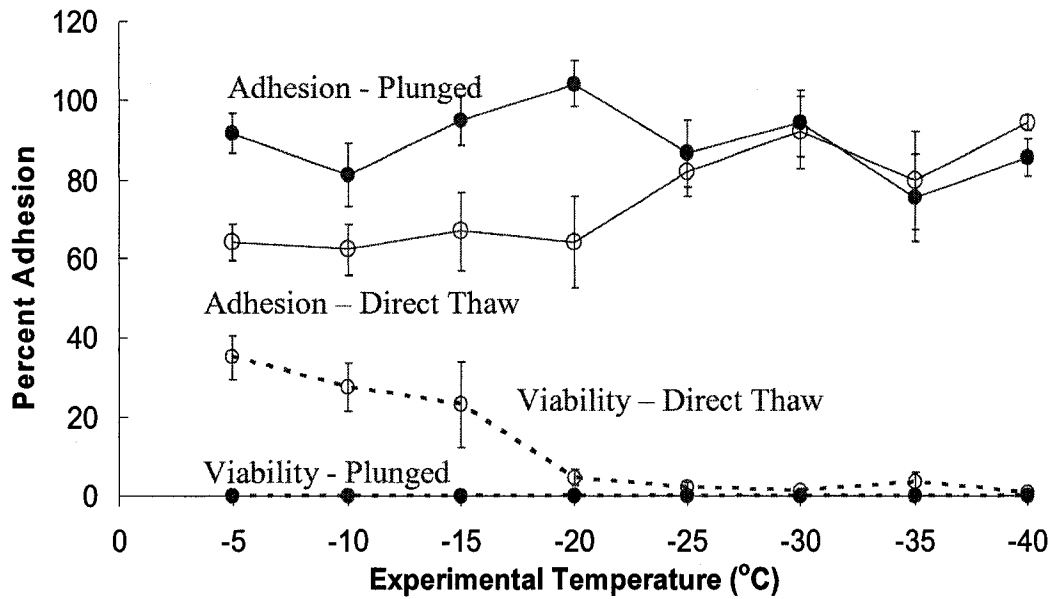


Figure 6. Previous data for 1 M DMSO showing a comparison of direct thaw and plunge conditions. Solid lines indicate adhesion and dotted lines indicate viability. Open circles represent direct thaw samples and closed circles represent plunged samples.

Figure 7 visually demonstrates the difference in adhesion of 1M DMSO treated samples between directly thawed samples or samples plunged to  $-196\text{ }^{\circ}\text{C}$ . Good adhesion is visible in plunged samples both at  $-5\text{ }^{\circ}\text{C}$  and  $-25\text{ }^{\circ}\text{C}$  as well as thawed samples at  $-25\text{ }^{\circ}\text{C}$ . While the direct thaw samples at  $-5\text{ }^{\circ}\text{C}$  maintained viability, adhesion was decreased and a patchy cell distribution was observed. Viability and adhesion were assessed for DMSO control samples, data not shown, and found to not be different than non-DMSO treated control samples.

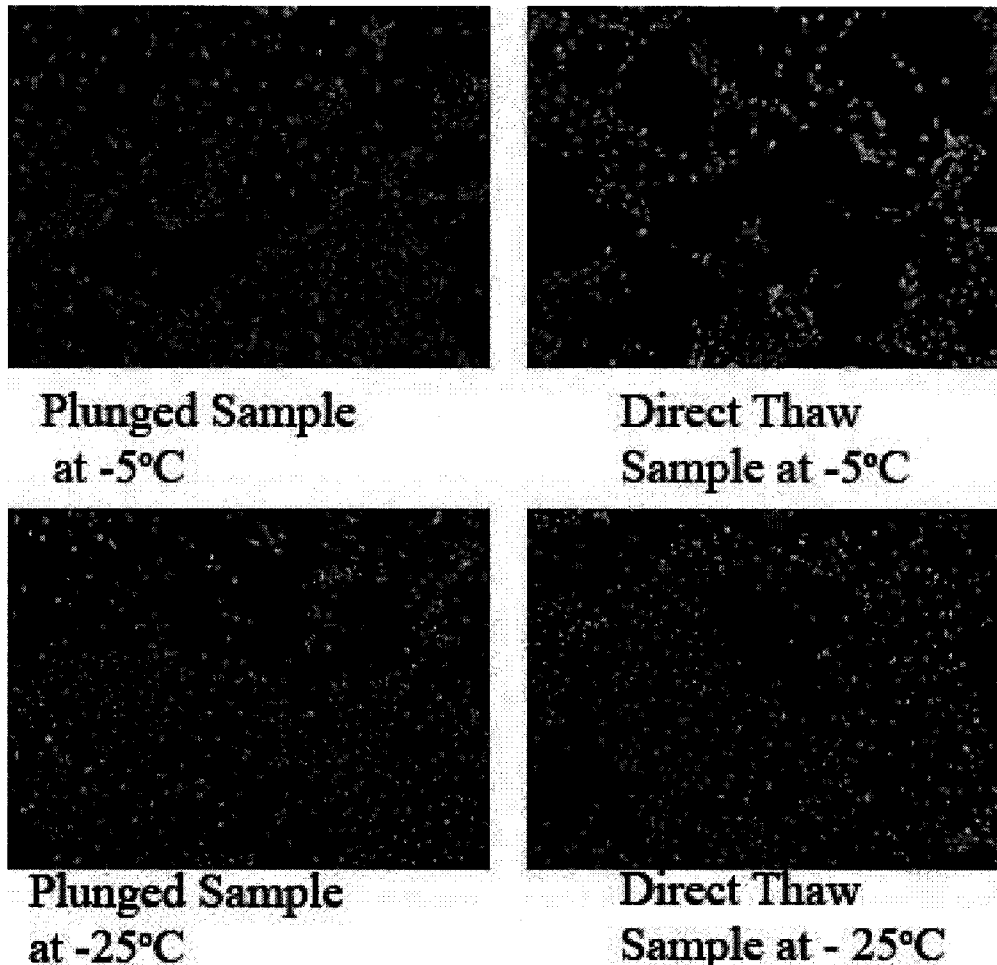


Figure 7. Representative samples thawed directly or plunged to  $-196\text{ }^{\circ}\text{C}$  from holding temperatures of  $-5$  and  $-25\text{ }^{\circ}\text{C}$ . Adhesion is increased in samples plunged to  $-196\text{ }^{\circ}\text{C}$  and direct thaw samples for experimental temperatures below  $-25\text{ }^{\circ}\text{C}$ . Plunged images are contrasted with the direct thaw condition at  $-5\text{ }^{\circ}\text{C}$  which shows increased viability, however adhesion is decreased. All images are for 1 M DMSO graded freezing samples.

## **Discussion**

### **Thermal Characteristics of the System**

A temperature profile was designed based on the experimental system used for the graded freezing protocol. Sample temperature was measured as a function of time in a  $-5\text{ }^{\circ}\text{C}$  bath, and the time after nucleation required for the sample to reach the initial bath temperature, and the subsequent time for removal of the latent heat of fusion after ice nucleation and cooling back to  $-5\text{ }^{\circ}\text{C}$ , were determined. The time selected for cooling of samples to  $-5\text{ }^{\circ}\text{C}$  in the bath was 3 minutes, before ice nucleation of the samples, to ensure all samples had reached the desired temperature. Six minutes post-nucleation was selected to ensure dissipation of latent heat of fusion and cooling back to  $-5\text{ }^{\circ}\text{C}$ . Data from this experiment using 20 mL scintillation vials and 1.5 mL of cell culture media was used to design the protocol for the following graded freezing experiments.

### **HUVEC Monolayer Response to Freezing**

Many studies have shown that cells in suspension respond differently to cryoinjury than cells in a monolayer. When frozen in the absence of DMSO, HUVEC monolayers retained low viability as the highest rate of recovery observed was  $\sim 25\%$  after direct thaw from  $-10\text{ }^{\circ}\text{C}$ , as shown in Figure 4. Viability declined to 0% recovery below  $-20\text{ }^{\circ}\text{C}$  during a direct thaw. Contrary to the deterioration in viability, adhesion was observed to steadily increase as the experimental temperature decreased for direct thaw samples. Plunged samples showed a similar trend of increasing adhesion but lower than direct thaw samples. There was no viability at any experimental temperature in plunged samples indicating cooling to  $-196\text{ }^{\circ}\text{C}$  is not well tolerated in HUVEC monolayers and rapid-cool injury is occurring.

HUVEC cells in suspension are routinely cryopreserved in 1 M DMSO and stored at  $-196\text{ }^{\circ}\text{C}$  with high post-thaw viability ( $\sim 70\%$ ). For cells in a monolayer, this study showed that 1 M DMSO confers very little cryoprotection of viability and may also be detrimental to adhesion for HUVEC monolayers after cooling at  $1\text{ }^{\circ}\text{C}/\text{min}$ . These experiments have shown the highest viability with 1M DMSO was approximately 35% after direct thaw from  $-5\text{ }^{\circ}\text{C}$  and the highest adhesion was approximately  $\sim 90\%$  after a

direct thaw from  $-30\text{ }^{\circ}\text{C}$ . Even in the presence of a cryoprotectant, DMSO, there was no viability in plunged samples for any experimental temperature.

Levels of adhesion were higher among non-DMSO treated samples compared to DMSO treated samples in the direct thaw condition. However, no difference was observed between DMSO and non-DMSO treated cells in the plunged to  $-196\text{ }^{\circ}\text{C}$  sample condition. Adhesion was also noted to be higher at low subzero temperatures for 1 M DMSO treated samples, both plunged to  $-196\text{ }^{\circ}\text{C}$  as well as direct thaw samples from experimental temperatures below  $-25\text{ }^{\circ}\text{C}$ , compared to DMSO treated monolayers thawed directly from  $-5\text{ }^{\circ}\text{C}$ . It appears DMSO slightly lowers cellular adhesion for direct thaw conditions at high subzero experimental temperatures when compared to non-treated samples. It was also observed that conditions which produced high adhesion, such as non-DMSO treated cells directly thawed or all conditions of plunge to  $-196\text{ }^{\circ}\text{C}$ , resulted in low viability. It was noted that conditions which maintained high adhesion correlated with conditions resulting in low viability. As shown in Figure 6, viability peaked at  $\sim 35\%$  at  $-5\text{ }^{\circ}\text{C}$  and steadily declined to  $0\%$  by  $-25\text{ }^{\circ}\text{C}$ , concurrently adhesion remained steady at  $\sim 65\%$  from  $-5$  to  $-20\text{ }^{\circ}\text{C}$  and sharply increased to above  $80\%$  below  $-25\text{ }^{\circ}\text{C}$ . As dynamic adhesion protein disassembly requires live cell signaling, we propose live cells post-thaw are capable of actively dissociating from the substratum while cells damaged as a result of the freezing process are unable to actively dissociate and therefore remain attached. This speculation explains the relationship observed where post-thaw maintenance of viability results in low cellular adhesion and low post-thaw viability is related to high adhesion.

Various mechanisms of injury could uniquely affect either viability or adhesion. Cellular shrinkage or mechanical damage caused by ice may be responsible for different types of cryoinjury which affect either viability or adhesion. Only one other known study has reported similar findings related to loss of monolayer adhesion (though not quantitatively) and viability; however no mechanisms were proposed regarding their findings to explain the results (3). One potential explanation could be cellular shrinkage resulting from diffusion of intracellular water during slow cooling at high subzero temperatures. As intracellular water diffuses across the membrane, concentrating intracellular solutes, the cell volume is adequately reduced to avoid intracellular ice

formation. However, the reduction in cell volume would reduce the surface area of cell-to-extracellular matrix contact. Weak cell junctions may be inadequate to maintain cellular attachment to the surface, resulting in a condition which maintains post-thaw viability but decreased cellular adhesion. This data is supported by a theoretical model and current data which indicates contractile forces, which occur during cell volume reduction, may promote the release of adhesions at the cell rear by physically rupturing weak or weakened molecular interactions driving adhesion disassembly (42). Our experimental results highlight that individual preservation protocols are responsible for maintaining either viability or adhesion in HUVEC monolayers. Further work is required to develop other preservation techniques capable of preserving both adhesion and viability. Alterations in the preservation protocol involving cooling rate, cryoprotectant used or thaw rate and further investigation into adhesion protein response to low temperature exposure may be required to understand and protect cell viability as well as cellular junctions responsible for cell-surface adhesion.

#### Insight Gained from a Graded Freezing Protocol

The use of a graded freezing protocol was selected to distinguish damage induced as a result of rapid-cool versus slow-cool injury. Samples directly thawed from the experimental temperature indicate damage during cooling at 1 °C/min to that temperature where cells are progressively shrinking as a result of exposure to increasing extracellular solute concentrations. Samples plunged from the experimental temperature to -196 °C show additional damage that must be indicative of rapid-cool injury. Damage may be occurring during rapid-cooling where intracellular water becomes increasingly supercooled as the sample temperature decreases. The resulting increase in supercooling increases the probability of intracellular nucleation and intracellular ice formation. One might normally expect that slow-cooling with a direct thaw could produce monolayers with relatively high post-thaw viability and maintenance of cellular adhesion. The literature indicates maximal cell recovery for cell suspensions from a graded freeze plunge condition occurs at ~-25 °C, with lower recovery at higher subzero temperatures, in the presence of DMSO (64). Another article indicated a viability of 79% following a 1 °C/min cooling rate to -80 °C and storage in liquid nitrogen for HUVEC suspensions in

the presence of 10% DMSO (36). We expected as monolayers were cooled to high to midrange experimental temperatures, cells would shrink sufficiently; avoiding intracellular ice formation as they were plunged to  $-196^{\circ}\text{C}$ . The results of our graded freezing experiments indicate rapid-cool injury is occurring in plunged samples as there was no retention of viability after exposure to  $-196^{\circ}\text{C}$  regardless of the presence of a cryoprotective agent. Damage was also observed in direct thaw samples; however there was some preservation of viability while adhesion was decreased. The loss of viability at low subzero experimental temperatures in direct thaw samples indicates cells are dying before being plunged. Related to the theory of cell injury proposed by Meryman, cell-to-cell and cell-to-surface interactions within monolayers limit the ability of the cells to shrink freely in response to the concentration gradient. As the osmolality increases with increasing ice formation an osmolality gradient develops across the plasma membrane which exceeds the tolerance of the membrane resulting in irreversible changes in membrane permeability and membrane damage (17, 18). Future work is required to develop a preservation condition which avoids the destruction of cell junctions during slow-cooling while still retaining cell viability by avoiding intracellular ice formation at more rapid cooling rates.

#### The Effectiveness of DMSO as a HUVEC Monolayer Cryoprotectant

No viability was observed in plunge samples with or without DMSO. However, 10% DMSO and a  $1^{\circ}\text{C}/\text{min}$  cooling rate are routinely used in preservation of HUVEC suspensions, often at  $-196^{\circ}\text{C}$ , with high post-thaw viability. Other tissues have also been found to respond favorably to DMSO including: articular cartilage which was found to recover from graded freezing plunge conditions with a maximal recovery of approximately 50% (65). Experiments using human corneal endothelial cell (HCEC) have also shown less than 10% recovery of viability in similar graded freezing experiments after plunging to  $-196^{\circ}\text{C}$  from any experimental temperature in the presence of 1 M DMSO. However, monolayers of those cells frozen in 1 M DMSO during a direct thaw resulted in virtually 100% membrane integrity and little detachment at all experimental temperatures, indicating slow cool injury is not a contributing factor to the loss of viability of HCEC monolayers during freezing and thawing (3). Preservation of

human corneas in 10% DMSO and a cooling rate of 1 °C/min indicated recovery of 70-90% of the endothelium (66). Even preservation of HUVEC suspensions in 10% DMSO and a cooling rate of 1 °C/min and storage in liquid nitrogen demonstrated a 79% post-thaw recovery (36). Although DMSO is an effective cryoprotectant for HUVEC suspensions and various other cell types, DMSO was found to be ineffective for the preservation of viability in HUVEC monolayers in this study.

DMSO did not significantly improve cell viability compared to non-DMSO treated monolayers at high subzero experimental temperatures, from -5 to -20 °C, and below -25 °C did not confer any protection to HUVEC monolayer viability. Supporting these results a study found that suspension cells are more resistant to DMSO than monolayers and over 50% of the intact endothelium was damaged or lost when exposed to 20% (w/w) DMSO at 4 °C, while the same treatment had no effect on cells in suspension (61). This paper suggested a role of either cell-cell or cell-matrix interactions in DMSO toxicity (61). In light of these results, we considered DMSO itself may be damaging to cellular integrity; however, examination of DMSO treated control samples relative to non-DMSO exposed control samples (data not shown) revealed that cells were unaffected in both adhesion and viability. These results indicate that DMSO is not itself toxic to the cells but is ineffective at protecting monolayers from freezing-induced damage.

As DMSO confers cryoprotection to HUVEC in suspension but not in a monolayer, this discrepancy may be related to intracellular ice formation in the monolayer. One study identified propagation of intracellular ice between adjacent cells through cell-cell junctions, but reported that intracellular ice formed under these conditions does not result in loss of viability (23). Based on previous work examining osmolality parameters of endothelial cells, it was found  $L_p$  (0.144  $\mu\text{m}/\text{atm}/\text{min}$ ) is low indicating a reduced plasma membrane permeability to water (67). Water transport across the membrane is further limited by cell-surface and cell-cell interactions which decrease the cell surface area available for diffusion. As the cells become supercooled as the temperature decreases, spontaneous nucleation in one cell facilitates nucleation in adjacent cells, resulting in intracellular ice injury across the monolayer (23). In light of the results presented above, we suspect intracellular ice formation occurred as HUVEC

monolayers were cooled below  $-25\text{ }^{\circ}\text{C}$  in the presence and absence of DMSO, and in all plunged samples, resulting in destruction of membrane integrity and viability. We believe as intracellular ice formation destroys the plasma membrane, cellular remnants remain adherent to the coverslip, appearing as dead cells, accounting for the high adhesion observed as viability decreases. A slightly higher direct thaw viability in DMSO treated samples could be explained as DMSO reduces the amount of ice formation at high subzero temperatures. Cellular suspensions are protected from this mechanism of injury as intracellular ice formation in one cell does not propagate to the rest of the cells, resulting in individual rather than multiple cell injury.

#### Hypothesis Related to Cellular Adhesion

A patchy cell distribution was also observed in some experimental conditions. Directly thawed cells were observed to maintain attachment in small cell clusters surrounded by large areas of cellular detachment. This phenomenon was observed down to an experimental temperature of  $-25\text{ }^{\circ}\text{C}$  for both DMSO and non-DMSO treated monolayers; however at lower experimental temperatures detachment was random. Previous studies of vascular preservation have also reported patchiness with areas of intense endothelial layer loss interspersed by zones where cells are well preserved; however they did not explain their findings (68). The strength of the intercellular connections may be one theory which could explain this patchiness phenomenon. It has been proposed that the strength of the cell-cell interactions may exceed the strength of the cell-surface interaction, so that cells in a monolayer detach more easily from the substrate during cryopreservation than from other cells (69). To investigate cellular interactions a study investigated single-attached and monolayers of mouse fibroblast cells (69). It was reported that single-attached cells, which lack cell-cell interactions, are more strongly attached while monolayers were more fragile and often tended to detach (69). Another author's speculation involves the effects of DMSO which cause a retraction of the apical cell membrane due to the generation of strong cortical tension, due to cell shrinkage, causing tension and ultimately gap formation between cells (70). We believe at high subzero temperatures cellular shrinkage occurs reducing cell height above the cell surface without disturbing cellular width and intercellular connections. However, as cells are

cooled further cell volume is lost across the width of the cells, causing cell walls to retract and break intercellular connections. The maintenance of cell-cell connections and weak cell-surface interactions could be responsible for increasing multiple cell detachment, therefore producing patchiness at high temperatures as cells detach in sheets. While these theories have been provided as hypotheses based on the observed findings, no conclusions regarding the cause of detachment or patchiness could be reached.

### **Conclusions**

Measured temperature profiles in experimental samples showed that the time required for the experimental system to reach the desired bath temperature of  $-5^{\circ}\text{C}$  should be approximately 3 min to ensure all samples reached the bath temperature. Samples were then nucleated and it was determined that 6 min was sufficient to ensure the latent heat of fusion had dissipated and the sample temperature returned to  $-5^{\circ}\text{C}$ . Based on these data, a graded freezing protocol was developed and used for all subsequent experiments.

Successful cryopreservation of blood vessels and corneas, where monolayers of endothelial cells are vital to function, require protection of both cell viability and cell adhesion. Based on the results of these experiments it appears that the protection of each will require different strategies. Freezing of endothelial monolayers using a graded freezing protocol produces significantly different results compared to freezing of cell suspensions, with significant evidence indicating HUVEC monolayers cannot be successfully preserved using conventional approaches. HUVEC monolayers are quite different from HUVEC suspensions as it was noted viability was lost after thawing from the highest subzero temperature tested. The most commonly-used cryoprotectant, DMSO, was found to protect neither viability nor adhesion to a significant degree in HUVEC monolayers during a graded freezing protocol cooled at  $1^{\circ}\text{C}/\text{min}$  for both direct thaw and plunge to  $-196^{\circ}\text{C}$  conditions. DMSO is an ineffective cryoprotectant for HUVEC monolayers under these conditions. A comparison with DMSO exposed non-frozen control samples shows that injury in HUVEC monolayers results from freezing damage and not DMSO toxicity. A graded freezing protocol was used not only to study the effects of slow-and rapid-cool injury on monolayer viability but also to identify

conditions leading to the loss of adhesion. Discrepancy in the conditions required to preserve adhesion and viability were identified indicating that it is difficult to maintain the integrity of both in one preservation protocol. The uniquely different and opposite cellular response to experimental conditions indicates multiple preservation strategies are required to cater separately to adhesion and viability. An inverse relationship between adhesion and viability was observed under all conditions and it was speculated live cell detachment was occurring. Contrarily high adhesion was noted among dead cells as they were unable to actively dissociate. Intracellular ice formation through intercellular junctions is speculated to be the cause of low post-freezing viability and high adhesion as cellular remnants were unable to detach. It was determined that an experimental protocol must be developed using conditions between slow-cool and rapid-cool to adequately preserve HUVEC monolayers. We hypothesized cell-cell adhesion may be stronger than cell-surface adhesion, producing the patchiness patterns observed at high subzero temperatures. While several speculations regarding cell detachment were presented, no conclusion regarding detachment and patchiness could be reached.

## **Chapter 5 – Influence of Prior Osmotic Shrinking on Graded Freezing Response**

### **Introduction**

As a result of an investigation in to the use of several pre-treatment solutions and their effects on post graded-freezing viability and adhesion a new experimental protocol was designed. An increase in post-thaw viability was noted with one solution indicating prior exposure to hypertonic solution was responsible for an increased post-thaw viability in monolayers.

Several theories relating to cellular response to hypertonic solutions are presented in the literature. Cells shrink in response to increased extracellular osmolality. However, damage may result when the cell volume is decreased beyond the minimum tolerable limit (17, 18). Lovelock suggested elevated salt concentrations increase the risk of cell injury by sequential thermal or mechanical stresses, while high salt concentrations were found to cause injury as a result of salt denaturation of membrane components (19). Other authors suggest the osmolality increases the stress of a fall in temperature causing a leakage of solutes, a phenomenon called thermal shock (71, 72). Another theory has suggested damage occurs during thaw following hypertonic exposure (19, 72). The cell membrane becomes leaky to solutes during the hypertonic phase of freezing leading to uptake of extracellular solutes; in an effort to re-equilibrate the osmotic gradient, water diffusion into the cell becomes damaging due to swelling upon thaw (72).

However, contrary to these theories, hypertonic exposure may not be entirely responsible for cell damage and effects appear to be concentration dependant. Hypertonic exposure of red blood cells in 1, 1.2 and 1.5 M concentrations of NaCl at 25 °C for 90 minutes without cooling found a 98.8, 97.9 and 96.5% recovery, respectively (73). While these findings indicate NaCl alone is not responsible for cell death, it has been suggested that the increased concentration of NaCl may render cells more susceptible to damage during rapid cooling (73). In addition, experimental evidence summarized by Meryman led to the hypothesis that water loss and volume reduction rather than any absolute ionic or solute concentration are responsible for the hypertonic injury associated with freezing (18).

In contrast, evidence presented in the literature has suggested exposure to increased osmolality solutions either during or prior to freezing can have beneficial effects on post-thaw recovery. Tenchini et al. found human embryonic epithelium cell solutions exposed for even a short period (24 h) to permissive hypertonic conditions (0.356 M NaCl) became resistant to more drastic hypertonic solutions (0.574 M NaCl) which normally would be incompatible with survival (74). They suggest the tolerance of these adapted cells to relatively high salt concentrations is likely to provide protection against freezing injury resulting from solution effects (74). Experiments using bull spermatozoa frozen in hypotonic, isotonic and various degrees of hypertonic solutions found the highest post-thaw motility and membrane integrity when frozen in moderately (1.5-2x isotonic) hypertonic solutions (75). These authors suggested pre-freeze shrinkage in hypertonic solutions was responsible for preventing intracellular ice formation and resulting cell death (75). A similar study investigated the effects of hypertonic exposure in cell suspensions and adherent cells (47). It was determined that in the absence of freezing, attached cells had a higher survival rate as a function of cation flux across a reduced membrane surface area (47). However, when freezing was performed, suspension cells fared better than attached cells indicating other mechanisms of damage occur during freezing (47). Despite these findings, to the best of this author's knowledge, no literature has been developed to investigate the role of pre-shrinkage in hypertonic solutions followed by return to isotonic conditions prior to freezing in confluent cell monolayers.

Based on validation from the investigative experimental protocol and evidence indicating hypertonic exposure is not exclusively damaging to cellular integrity, it was determined that 2x PBS produced optimal cell recovery following a graded freezing procedure. As a condition which maintained post-preservation viability had potentially been identified, further investigation into hyperosmotic exposure of HUVEC monolayers was required to determine if viable HUVEC monolayers could be preserved. It was therefore decided to further investigate the cellular response of exposure to 2x PBS alone and in the presence of DMSO to determine if an optimal freezing protocol for HUVEC monolayers could be produced. The objectives of this chapter were to investigate the effects of prior hypertonic exposure on viability and adhesion of HUVEC monolayers using the graded freezing procedure with and without DMSO.

## **Materials and Methods**

### **Cell Preparation**

HUVEC were cultured in EBM-2 cell culture media at 37 °C and 5% CO<sub>2</sub> in 75 cm<sup>2</sup> flasks (VWR) until cell density reached 70% as described in Chapter 3. Cells were passaged with 0.25% trypsin-EDTA (Gibco) and 600,000 cells were plated on fibronectin coated coverslips and incubated for 7 to 9 days to form confluent monolayers.

### **Condition Screening Experiment**

To determine if treatment with various cell solutions increased post-thaw viability, an experiment was performed. Cell samples were individually exposed to one solution, combinations of solutions or a variability of time. The primary variables were the presence of DMSO, Bovine Serum Albumin (BSA) and prior hypertonic exposure.

All samples excluding control samples were exposed to a 10 minute incubation in 1 M DMSO at room temperature. Samples were then exposed to a graded freezing protocol down to -10 °C followed by a direct thaw at 37 °C. A temperature of -10 °C was selected as this temperature allowed cellular exposure to the graded freezing protocol with cooling at 1 °C/min and high post-thaw viability was expected based on the results from Figure 4 in Chapter 4. Viability and adhesion were assessed by SYTO/EB staining and imaging as described in Chapter 2.

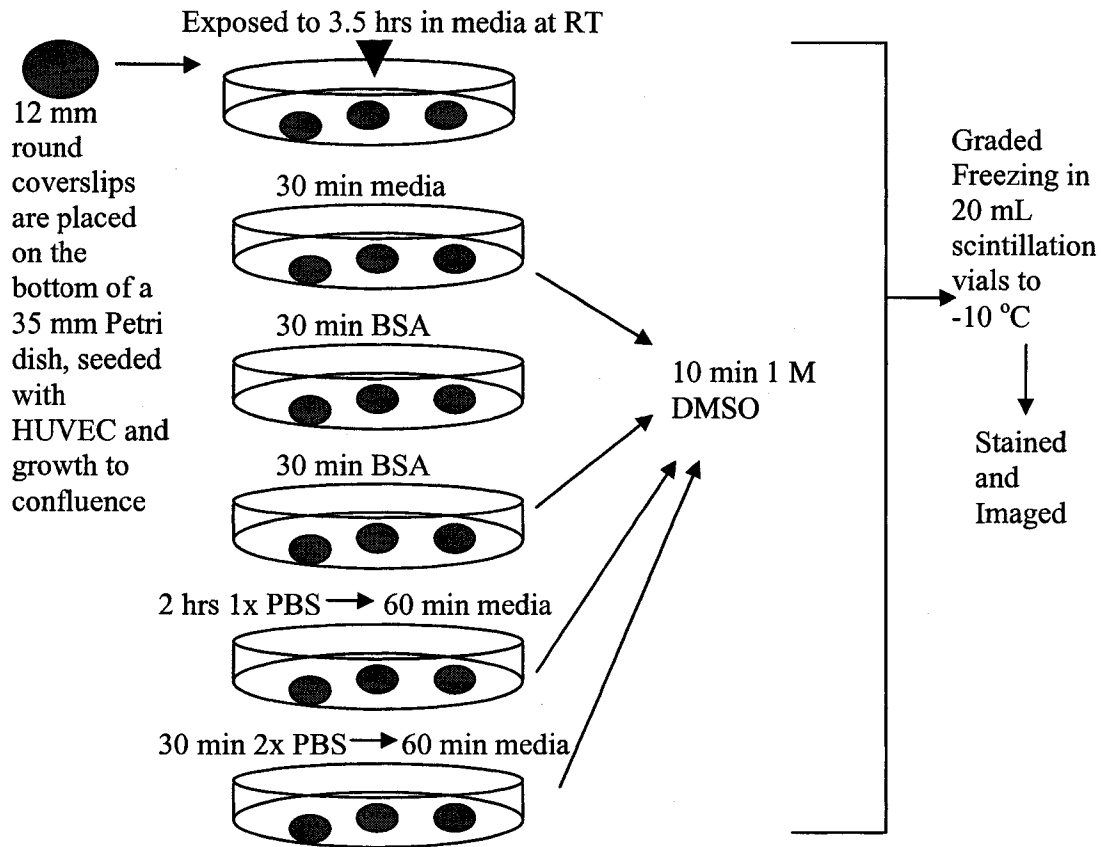


Figure 1. Schematic diagram of conditions screening experiment.

#### Prior Hypertonic Exposure in 2x PBS

For 2x PBS exposed experimental conditions, cell monolayers were preshrunk in 2x PBS at room temperature. A shorter hold time, referred to as “short hold”, of 5 minutes in 2x PBS followed by 5 minutes in media at room temperature was selected to rule out hypertonic toxicity with a 30 minute exposure. “Long hold” refers to 30 minutes in 2x PBS followed by 1.5 hrs in media at room temperature. Using a freezing point depression method an osmometer was used to make osmolality measurements. Measures of osmolality indicated EBM-2 culture media has an osmolality of 284 mOsm, 1x PBS was 281 mOsm and 2x PBS was 582 mOsm.

Cells were returned to isotonic conditions by replacing the 2x PBS solution with cell culture media for 1.5 hours at room temperature followed by the addition of 1 M DMSO to the culture media and an incubation of 10 minutes at room temperature before the graded freezing procedure was performed. For conditions requiring 2x PBS but no

DMSO, the 10 minute incubation with 1M DMSO was omitted. Graded freezing experiments were performed as previously described in Chapter 4. Cells were stained for viability with SYTO/EB and imaged. Analysis was performed with Viability 3 for viability and adhesion.

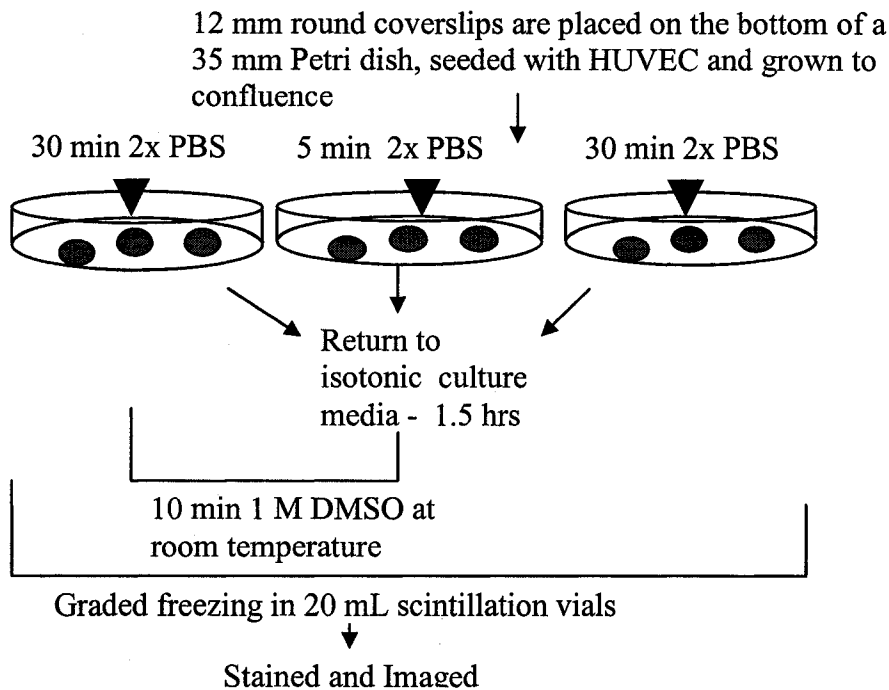


Figure 2. Schematic diagram of pre-shrinkage in 2x PBS prior to graded freezing protocol.

## **Results**

### **Validation Experiment**

Viability and adhesion were determined for each experimental treatment condition in order to identify the steps resulting in viability observed in a 1 M DMSO graded freezing procedure following cell exposure to integrin staining. Figure 3 shows that results obtained for monolayer freezing in culture media with no cryoprotectant correlate with previous graded freezing direct thaw results at  $-10^{\circ}\text{C}$  (Figure 4, Chapter 4). DMSO was found to increase viability ( $\sim 40\%$ ) compared to non-DMSO exposed samples ( $\sim 20\%$ ), again correlating with previous 1 M DMSO graded freezing experiments (Figure 4, Chapter 4). BSA alone did not provide any more protection to

cellular viability than cell media (both ~20%), however in conjunction with DMSO a sharp increase in viability was observed (~75%). Exposure to isotonic (1x) PBS prior to freezing with 1 M DMSO resulted in a viability of ~50%, comparable to freezing in DMSO alone. Adhesion was relatively consistent at approximately 75% for samples frozen in media, DMSO and BSA alone. An increase in adhesion was observed (~85-98%) when combination treatments were used including BSA and DMSO, pre-exposure to 1x PBS or 2x PBS followed by freezing in 1 M DMSO. Based on adhesion and viability measurements, exposure to 2x PBS followed by a return to isotonic solution and subsequent freezing in 1 M DMSO resulted in the greatest protection for both adhesion and viability (~98% adhesion and ~88% viability). Pre-shrinkage in 2x PBS showed a higher post-thaw recovery than DMSO alone. Based on these results, pre-shrinking in 2x PBS was selected to investigate further with graded freezing experiments in the presence and absence of 1 M DMSO.

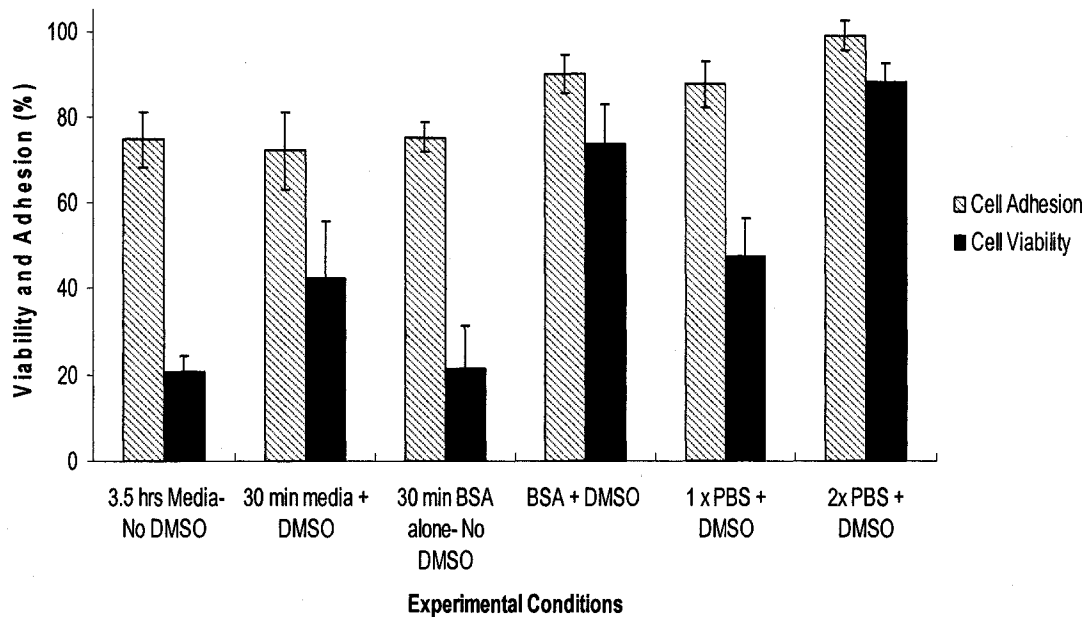


Figure 3. Graded freezing validation experiment using a direct thaw from -10 °C for various experimental conditions. Hashed bars represent cell adhesion and solid bars represent viability. Conditions included: equilibration for 3.5 hrs in culture media followed by freezing, equilibration for 30 min followed by freezing in 1 M DMSO,

equilibration for 30 min in BSA – no DMSO, 30 min equilibration in BSA followed by freezing with 1 M DMSO, exposure to 1x PBS for 30 min followed by return to isotonic media and freezing with 1 M DMSO and exposure to 2x PBS for 30 min followed by return to isotonic media and freezing with 1 M DMSO.

#### Cellular Viability and Adhesion Following 2x PBS Exposure

Figure 4 shows that pre-shrinkage in 2x PBS followed by a return to isotonic conditions and then graded freezing (direct thaw only) with 1 M DMSO had considerably increased viability at high subzero temperatures down to -30 °C compared to samples treated with DMSO alone and non-DMSO treated cells. Both long and short hold exposures to 2x PBS and subsequent return to isotonic and then freezing with DMSO resulted in high post-thaw viability (peaking at ~75%) for direct thaws indicating short term exposure to hypertonic solutions is as effective as longer exposures and long exposure is not toxic to the monolayers. Pre-shrinkage in 2x PBS alone was not effective at maintaining high post-thaw viability below -10 °C, reaching a peak of 65% at -5 °C and quickly dropping to ~28% by -10 °C . This data indicates that in conjunction, pre-shrinkage in hypertonic solution and freezing with DMSO down to -25 °C and directly thawing, effectively preserve viability at high subzero temperatures. However, each of pre-shrinkage and DMSO alone are ineffective at maintaining the same degree of post-thaw viability. All conditions indicate direct-thaw viability is strongly affected by temperature. Plunge to -196 °C conditions, data not shown, maintained no viability in any condition.

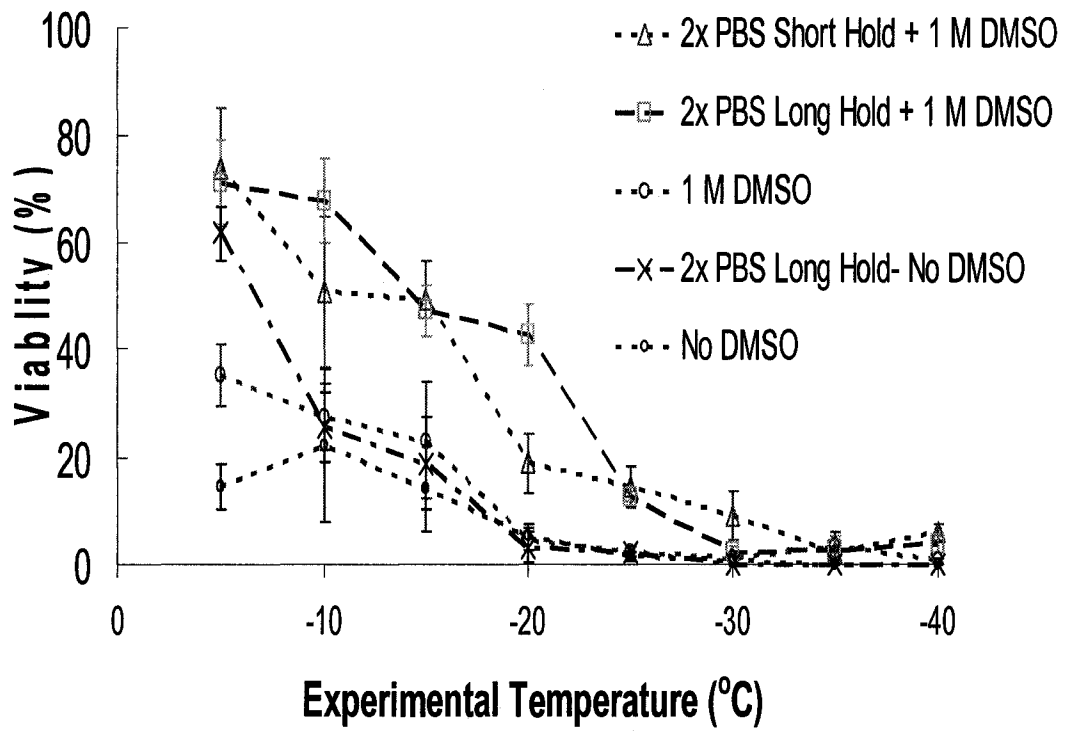


Figure 4. Comparison of viability following graded freezing direct thaw with 1 M DMSO and no-DMSO, DMSO alone, and no-DMSO treated samples of short and long hold pre-shrinkage in 2x PBS and a return to isotonic conditions.

Figure 5 shows post-thaw differences in adhesion are small and not notably affected by the experimental treatment. Unlike the results for viability, pre-shrinkage is not noticeably protective of adhesion at any experimental temperature and post-direct-thaw adhesion is not strongly temperature dependant. All conditions of 2x PBS and DMSO, 2x PBS alone and 1 M DMSO alone did not increase cellular adhesion following graded freezing direct thaw and plunge (data not shown) conditions. The trend presented in Figure 5, indicates non-DMSO treated cells maintain the greatest degree of adhesion, with increasing adhesion towards lower subzero temperatures.

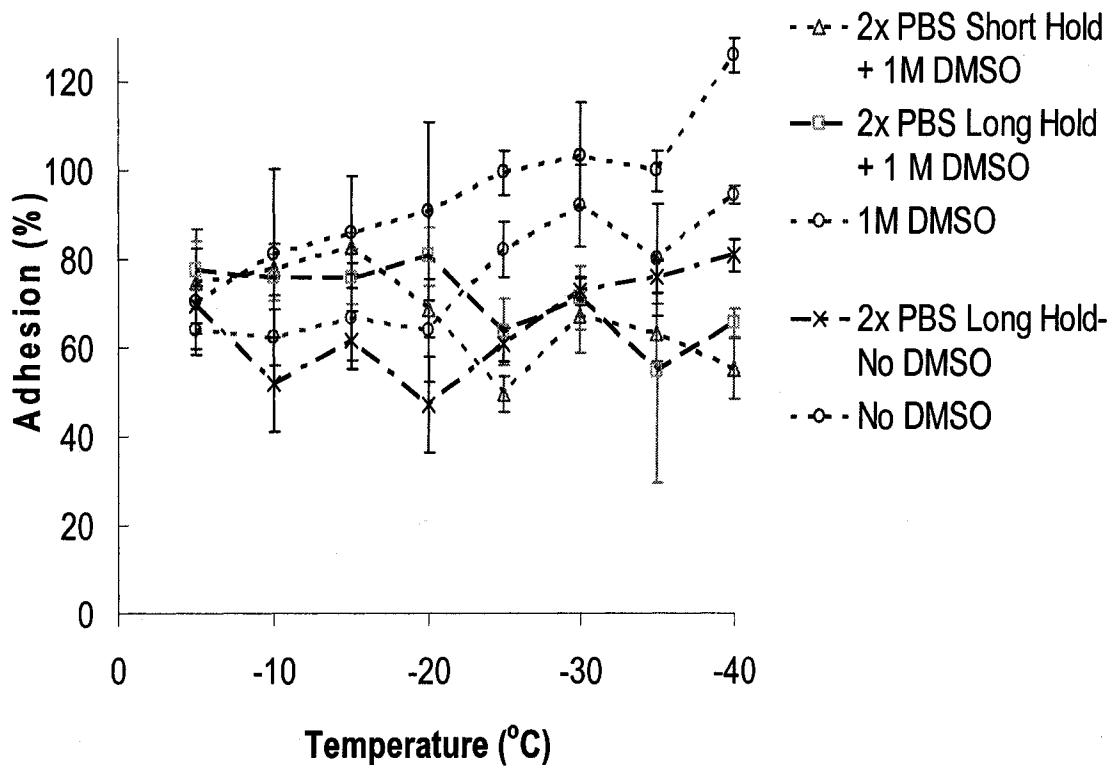


Figure 5. Comparison of adhesion following graded freezing direct thaw of short and long hold pre-shrinkage in 2x PBS with 1M DMSO and no-DMSO, DMSO alone, and no-DMSO treated samples.

### Discussion

Unexpected results of a grading freezing experiment using monolayers, exposed to an integrin staining protocol, provided motivation for further investigation to determine what steps in the integrin protocol were responsible for the increase in post-

preservation viability. Validation of experimental conditions, freezing in culture media alone and DMSO alone, correlated well with previous graded freezing experiments of the same conditions. Freezing in BSA alone was found to produce the same post-thaw viability as freezing in media alone (~20%), indicating BSA itself is not protective to HUVEC monolayers. However, a combination of BSA and DMSO resulted in significantly higher post-direct-thaw viability (~75%). Pre-freezing exposure of monolayers to 1x PBS followed by a return to isotonic culture media and freezing in DMSO showed viability comparable to freezing in DMSO alone, indicating exposure to 1x PBS did not affect post-thaw viability. The results of this experiment also indicated that prior exposure to a 2x PBS solution resulted in an increased post-direct-thaw viability to approximately 90% and post-thaw adhesion to approximately 98%. Adhesion was comparable among cells frozen in media, DMSO or BSA alone at ~75%; however combination treatments involving DMSO and BSA, 1x PBS or 2x PBS resulted in increased adhesion to ~90% or greater. The results of pre-shrinkage in 2x PBS provided optimism that an experimental condition which favors adhesion and viability had been found. Based on these results it was decided to continue investigating the effects of 2x PBS in long and short hold times, with and without 1M DMSO using a graded freezing protocol.

Graded freezing protocol experiments were investigated where cells were pre-shrunk with 2x PBS followed by a return to isotonic conditions before exposure to 1M DMSO and freezing. A long hold condition of 30 minutes was performed and a short hold of 5 minutes was added to rule out damage due to hypertonic exposure. Both 2x PBS with DMSO long and short hold times produced an increase in overall viability down to -30 °C, below which all conditions appeared to have no protective qualities for viability. It was determined that together PBS and DMSO increase viability in HUVEC monolayers, however, DMSO and PBS alone do not produce the same drastic increase in viability and are not considerably different from non-DMSO treated samples below -10 °C. This would indicate that there is a synergistic effect of pre-shrinkage and DMSO protection resulting in avoidance of freezing injury and maintenance of viability. While further investigation would be required to confirm our hypothesis, it is thought pre-shrinkage in 2x PBS results in cell volume reduction, stressing the intercellular junctions.

Cells are returned to isotonic conditions and return to isotonic cell volume, however, the intercellular junctions have been compromised and do not have sufficient time to reform prior to freezing. As intercellular bonds have been broken the propagation of intracellular ice among adjacent cells through gap junctions is limited preventing the degree of monolayer damage observed in Chapter 4. DMSO is thought to further increase cellular protection by lowering the freezing point, preventing spontaneous intracellular ice formation at high subzero temperatures. However, we believe the protective effects of pre-shrinkage and DMSO are lost at mid-to-low subzero temperature as intracellular ice spontaneously forms in individual supercooled cells.

Supportive theories suggest suspension cells exposed to hypertonic solutions during slow cooling become distorted and contorted but cells exposed to hypertonic solutions in absence of freezing shrink in an isotropic fashion (10). This theory suggests that physical forces other than osmotic gradients are present during freezing and cell injury may be a consequence of those forces (10). While pre-shrinkage helps preserve monolayer viability post-direct-thaw, exposure to 2x PBS did not protect post-direct-thaw adhesion. The maintenance of adhesion appeared to be highest among cells with no experimental treatment (neither 2x PBS nor DMSO), indicating prior cell shrinkage may induce cell detachment. This finding supports our theory that cellular detachment of live cells occurs post-thaw. While cells exposed to no experimental treatment had the highest post-thaw adhesion, they also retained the lowest post-thaw viability. It is believed 2x PBS and DMSO protected post-thaw viability allowing live cells to dissociate from the cell-matrix, reducing cellular post-thaw adhesion. DMSO may also be responsible for cellular detachment (previously discussed in Chapter 4). While DMSO exposure is likely not toxic to cellular viability it is thought to affect cell-to-cell and cell-to-matrix interactions (61).

This data suggests exposure to one stress at a time, cell shrinkage before freezing followed by a return to isotonic volume, is advantageous for post-direct-thaw viability. As cell-to-cell contacts are removed, cells behave more like single attached cells than cells in a monolayer and cellular detachment occurs as individual cells and not detachment in sheets. The destruction of intercellular interactions, as a result of

shrinkage, may also limit the propagation of intracellular ice nucleation resulting in reduced cellular injury compared to intact cellular monolayers.

### **Conclusions**

Prior exposure to hypertonic solution was found to be the most protective of adhesion and viability as a result of investigating the effects of an integrin staining protocol on graded freezing with 1 M DMSO. Exposure of HUVEC monolayers to 2x PBS for long and short hold periods with and without 1 M DMSO followed by a return to isotonic conditions, revealed 2x PBS with 1 M DMSO provided optimal viability post-direct-thaw. Pre-shrinkage of cells before freezing was found to increase cell viability allowing live cells to detach, subsequently increasing the rate of detachment. There was found to be a synergistic effect of DMSO and 2x PBS which resulted in higher post-thaw viability than DMSO or PBS alone. It is thought pre-shrinkage with 2x PBS breaks intercellular connections responsible for propagating intercellular ice nucleation within the monolayer. Destruction of these junctions allows adherent cells to behave more like individual cells in suspension. DMSO is thought to further protect cells by lowering the point of spontaneous intracellular nucleation, avoiding intracellular ice formation damage at high to moderate subzero temperatures. Increased adhesion but no viability was found among plunge samples and was determined to be likely due to the disruption of cell-cell interactions and intracellular ice formation, likely resulting in destruction of the plasma membrane, resulting in cell death and an inability of cells to detach. The result of these experiments suggests that adhesion and viability are independent variables which require independent and unique preservation conditions to maintain monolayer functionality.

## **Chapter 6 – General Conclusions**

### **Experimental Conclusions**

As a result of the presented experiments it is clear that HUVEC monolayers have a unique response to freezing compared to cells in suspension. In order to determine a HUVEC monolayer's response to cryopreservation, experimental objectives were developed and carried out. Justification of experimental assessment techniques was performed to ensure the experimental techniques developed accurately represented cell viability and adhesion. The membrane integrity stains used (SYTO and ethidium bromide (EB)) were previously validated and justified to be effective and appropriate cell viability markers (50). SYTO was found to localize to individual cells in the sample, allowing determination of viability in individual cells and detection of viability patterns and adhesion. Microscope camera settings were adjusted and optimal parameters were identified which consistently produced quality images for reproducibility of image analysis software.

Cell analysis software Viability 3, previously developed by Dr. Locksley McGann, was assessed and determined to be appropriate and reliable for the experimental system. Manual cell counting of images was compared with Viability 3 analysis of the same images and was used to justify the analysis software. A small margin of error was produced by the program; however, the error actually moderately reduces the percentage of viability and adhesion by 5%, indicating results may be conservative since successes are undercounted by the program. It was also determined that use of the analysis software was more consistent and accurate than manual analysis of several images, removing human error (51). Using information provided by the program, absolute viability and adhesion were preferentially determined. Contrary to relative viability, absolute viability more accurately represented cell viability and adhesion relative to control images, taking into account experimentally induced detachment. To the best of the author's knowledge there are no other accounts reported in the literature where viability and adhesion were simultaneously quantitatively analyzed. Previous analysis of Human Corneal Endothelial Cells with SYTO/EB by Ebertz and McGann used custom cell analysis software to determine viability; however qualitative grading scales were used to assess adhesion (3).

In order to investigate cell monolayer interactions *in vitro* cell monolayer models were used. HUVEC were chosen as adult endothelium *in vivo* is one of the few cell types that is a single cell layer thick (49). For optimal cell growth cell substrate fibronectin was chosen to coat the cell culture surface. A concentration of  $10 \mu\text{g}/\text{cm}^2$  of human plasma fibronectin was determined to be optimal for cell growth within a 48 hour culture period. A comparative examination of fresh versus stored fibronectin-coated coverslips at  $4^\circ\text{C}$  indicated that the use of stored fibronectin-coated coverslips was acceptable.

To ensure cell-cell junctions and cell-surface interactions were present, the development of a confluent HUVEC monolayer model was paramount to the experimental system. To determine when a level of confluence was reached both qualitative and quantitative analysis methods were used. Cell viability and adhesion were determined from a growth curve and analysis of morphology was determined using phase contrast microscopy. Quantitative assessment of adhesion and viability was performed using SYTO/EB staining and Viability 3 software while qualitative assessment of morphology revealed when the characteristic cobble-stone morphology had been reached. A combination of qualitative and quantitative analysis revealed a time period from 7 to 9 days was optimal for experimentation with confluent HUVEC monolayers. The contribution from and agreement between both qualitative and quantitative methods of analysis suggests that both methods should be used to assess confluence in HUVEC monolayers.

In an effort to determine the conditions under which HUVEC cells remained attached and remain viable it was necessary to first determine the most suitable graded freezing protocol for the experimental system. A temperature profile of the experimental system was performed and indicated 3 minutes was sufficient for the sample to reach the bath temperature and 6 minutes was required to ensure the latent heat of fusion had fully dissipated. These values were incorporated into the graded freezing protocol and were used for each graded freezing experiment.

A graded freezing experimental protocol was selected to distinguish between rapid- or slow-cooling induced cellular damage. Graded freezing in the absence of DMSO indicated HUVEC monolayers retained low viability (peaking at  $\sim 25\%$  at direct-thaw  $-10^\circ\text{C}$ ) while adhesion was found to steadily increase as the experimental

temperature decreased; an adhesion trend was also observed in plunged samples. Graded freezing with 1M DMSO was found to not noticeably improve HUVEC survival in direct thaw conditions (peak viability was ~35% at -5 °C); however, adhesion was once again observed to increase as experimental temperatures decreased. Viability was completely destroyed in all plunged samples. It was noted that high adhesion and viability are inversely correlated. It was speculated that protection of cell viability allowed live cell signaling pathways to induce cellular dissociation from the matrix. As dissociations of adhesion proteins is an active process, cells damaged by cryoinjury at low subzero temperature or during the plunge condition would be unable to actively detach from the cellular matrix, increasing post-thaw adhesion.

Use of a graded freezing protocol allowed for the identification of cell damage as either slow-cool or rapid-cool injury. No retention of viability was observed among plunged samples indicating rapid-cool injury (i.e. intracellular ice formation) may be responsible for killing HUVEC monolayers. However, cell death was also observed in direct-thaw samples at low subzero temperatures indicating cell death is occurring prior to rapid-cool plunge. One possible explanation could involve membrane damage as result of osmolality gradients during slow-cooling.

Adhesion and viability were not protected by DMSO in the direct thaw samples and there was absolutely no protection of viability among plunge samples. It was determined that 1 M DMSO did not protect HUVEC monolayers as it protects cells in suspension; therefore it was concluded 1 M DMSO is an ineffective cryoprotectant for HUVEC monolayers cooled at 1 °C/min in a graded freezing protocol. Suspicion indicated DMSO may be toxic to intercellular junctions; however analysis of DMSO treated control samples found no evidence of DMSO toxicity, therefore ruling it out as a cause of poor viability. We believe the source of cellular injury is intracellular ice formation resulting from intercellular nucleation via gap junctions. As endothelial cells are known to have a low membrane permeability to water, intracellular water may not diffuse quickly enough from the cell. The remaining intracellular water becomes increasingly supercooled as the temperature increases, increasing the probability of nucleation. At high subzero temperatures a wave of propagating intracellular ice may spread between gap junctions of firmly bonded cells; however at low subzero

temperatures, spontaneous nucleation could occur damaging all cells regardless of cell junctions. It is possible to speculate that the high adhesion rate observed in plunge samples is likely representative of the cell membrane no longer remaining intact, leaving the membrane shell on the surface, explaining the absence of viability within the plunge samples. Direct thaw samples likely retain an intact membrane and detachment is probably of live cells. We believe damage to HUVEC during preservation may be a result of various sources of freezing damage which DMSO does not provide protection against. These results indicate future work should examine a non-permeating cryoprotectant to determine if various other cryoprotectants provide greater protection of viability and adhesion.

A patchiness phenomenon of cellular detachment was also observed in 1 M DMSO and non-DMSO treated cells at higher temperatures during direct thaw. It is thought that cell-surface adhesion is weaker than cell-cell adhesion, indicating individual cells may be detaching and pulling adjacent cells with them. The results of this work clearly illustrate the individual cellular characteristics of adhesion and viability in response to different cooling conditions. It is clear that new preservation strategies need to be developed which optimize the maintenance of both adhesion and viability to retain normal tissue functionality. These findings indicate that HUVEC monolayers do not behave the same as other monolayer models.

The effects of osmolality on cell membranes and shrinkage have previously been discussed within the literature. Meryman proposed mechanical resistance to volume changes in living cells, where there is a resistance to shrinkage, leads to the development of an osmotic pressure gradient across the membrane as the interior is at a lesser pressure than the exterior (18). He speculated this pressure gradient may be responsible for membrane damage during hypertonic stress (18). It was also stated that water loss and volume reduction rather than absolute ionic concentration are responsible for hypertonic associated injury during freezing (18). An initial exploration of pre-cryopreservation hypertonic shrinkage of HUVEC monolayers was motivated by a failed attempt to stain surface integrins followed by graded freezing with 1 M DMSO. An above average increase in viability and adhesion in 1 M DMSO graded freezing experimental cells prompted further investigation. A follow up experiment revealed cellular pre-shrinkage

in 2x PBS followed by return to isotonic produced the greatest post-thaw viability and adhesion following a graded freezing experiment with 1M DMSO from -10°C. A combination of bovine serum albumin (BSA) and DMSO was also found to increase adhesion and viability; however neither BSA nor DMSO alone could produce the same results.

Graded freezing experiments with pre-shrinkage in 2x PBS followed by freezing in 1M DMSO were explored and indicated an increase in viability (~70% at -10 °C). However this increase was determined to be due to a synergistic effect of PBS and DMSO as neither PBS or DMSO alone could replicate the increase in viability. Previous literature has suspected that pre-shrinkage without freezing of cells leads to shrinkage in an isotropic fashion (10). During slow cooling, increases in hypertonicity and a drop in temperature are occurring together and the thermal shock effect will induce damage at a lower osmolality than that required to induce leakage under constant temperature conditions (72). This author suspects that exposure to DMSO and PBS together increase viability as pre-freezing shrinkage may help to reduce intracellular ice formation while DMSO protects from other sources of freezing injury. However, there appeared to be no protection for cells in the plunge condition as no viability remained. Pre-shrinkage in 2x PBS and freezing with DMSO were not found to affect adhesion. On the contrary, the trend indicated samples treated with neither PBS or DMSO had the greatest remaining adherent cells.

Overall it is speculated that at lower temperature, below -25 °C, remaining live cells dissociate their cell surface interactions but retain cell-cell interaction and pull adjacent cells off in sheets accounting for the decrease in adhesion among pre-shrunk and DMSO treated cells. Conversely cells exposed to no experimental treatment succumbed to freezing injury resulting in no retention of viability and an inability of adhesion proteins to actively dissociation, accounting for the increase in post-thaw adhesion. Additional mechanisms of damage at low subzero temperatures could include post-hypertonic damage upon thawing resulting from excessive entry of water due to penetration of solute molecules during the hypertonic phase (72).

### **Limitations of Research**

Throughout the course of this thesis conditions that increased viability were determined; however we were unable to determine conditions of increased adhesion. Further research into a combination of experimental conditions which allow cell shrinkage without breaking cell-surface interactions is required. This set of experiments was also limited to one cell type and should be experimentally expanded to include various cell-type monolayers. Finally, the ineffectiveness of DMSO in monolayer preservation can only be concluded for HUVEC cooled at 1 °C/min and care should be taken not to generalize these findings to all monolayer models.

### **Future Research**

As HUVEC have a low  $L_p$ , 0.144  $\mu\text{m}/\text{atm}/\text{min}$ , a slower cooling rate may be more appropriate (67). The 1 °C/min cooling rate used within this experimental set may be too rapid, therefore a cooling rate of 0.1 °C/min may allow for the appropriate amount of cell shrinkage. As HUVEC also have a high activation energy, 14.5 kcal/mol, they may get ice formation as the temperature decreases and at lower temperatures experience increased supercooling which produces more intracellular nucleation (20). A study of intact rabbit corneas supports the use of slower cooling rates (below 1 °C/min) as they found it improved corneal endothelial cell recovery, maintained morphology and there was evidence of retained endothelial function (34).

Variation of HUVEC monolayer thaw rates could also be investigated to determine if thaw conditions improve viability or adhesion; however there are several conflicting reports of thaw rate presented in the literature. Bujan et al. suggested that slow thaw allows the structure of arterial vessels to be best preserved (32). In agreement, investigation of the common iliac artery of minipig found that slower thaw for endothelial cells led to improved morphological features and viability over rapid thaw (31). They found that rapid thaw produced irreversible ultrastructural damage such as mitochondrial dilation and rupture, reticular formation and peripheral nuclear condensation (31). While slow thaw showed changes that were more reversible such as general swelling, reticular dilation, mitochondrial swelling and nuclear chromatin condensation (31). Pascual et al. found that storage of endothelial cells at -80 °C

followed by a rapid thaw led to the greatest endothelial cell loss (61.36 +/- 9.06% covered endothelial surface) while temperatures of -145 °C and slow thaw best preserved vessel endothelium ( 89.38 +/- 16.67%) (31). However, it has been found after cooling at 1°C/min, that rapid warming is better than slow re-warming for hamster hearts (76). Further investigations on the effects of thaw rate are required with HUVEC monolayers to determine if a slow or rapid-thaw increases endothelium preservation.

Finally, an alteration in cryoprotectant used in the experimental protocol may improve preservation. Studies have found polyethylene glycol (PEG-400) to be the best cryoprotectant in the preservation of porcine corneas as it has low cytotoxicity and its presence hinders ice crystal formation (77). Similarly, another study compared freezing of human corneas at 1 and 5 °C/min in glycerol, DMSO and 1,2PD and PEG-400 (66). PEG-400 produced the most promising results (75-98% viability) (66). PEG has also been reported to reduce the deleterious effects of cold on the cytoskeleton (78). Further experimentation with various cryopreservative agents, both permeating and non-permeating, could reveal a cryopreservation technique capable of preserving both adhesion and viability.

The limitations of vessel and corneal preservation are restricted by the inability to preserve both adhesion and viability. The work presented above highlights the unique nature of HUVEC monolayers versus cells in suspension. The development of successful preservation protocols, capable of preserving the tissue integrity and function are required before advances in tissue banking can be achieved.

### References Cited

1. Han B, Bischof JC. Engineering challenges in tissue preservation. *Cell Preservation Technology* 2004;2(2):91-112.
2. Karlsson JOM, Toner M. Long-term storage of tissues by cryopreservation: Critical issues. *Biomaterials* 1996;17(3):243-256.
3. Ebertz SL, McGann LE. Cryoinjury in endothelial cell monolayers. *Cryobiology* 2004;49(1):37-44.
4. Muldrew KB, Acker J, Elliott JAW, McGann LE. The Water to Ice Transition: Implications for Living Cells. In: Fuller BJ, Lane N, Benson EE, editors. *Life in the Frozen State*: CRC Press; 2004. p. 67-108.
5. Hempling HG, Thompson S, Dupre A. Osmotic Properties of Human Lymphocyte. *Journal of Cellular Physiology* 1977;93(2):293-302.
6. Jacobs MH. The simultaneous measurement of cell permeability to water and to dissolved substances. *Journal of Cellular and Comparative Physiology* 1933;2:427-444.
7. Jacobs MH, Stewart DR. A simple method of quantitative measurement of cell permeability. *Journal of Cellular and Comparative Physiology* 1932;1:71-82.
8. Elmoazzen HY, Elliott JAW, McGann LE. The effect of temperature on membrane hydraulic conductivity. *Cryobiology* 2002;45:68-79.
9. Folger SH. *Elements of Chemical Reaction Engineering*. In. 4th ed: Prentice Hall; 2006. p. 91-99.
10. Mazur P. Freezing of Living Cells - Mechanisms and Implications. *American Journal of Physiology* 1984;247(3):C125-C142.
11. Mazur P. Physical and chemical basis of injury of single-celled micro-organisms subjected to freezing and thawing. In: Meryman HT, editor. *New York: Academic Press*; 1966. p. 214-315.
12. Muldrew KB, McGann L. Mechanisms of intracellular ice formation. *Biophysical Journal* 1990;57:525-532.
13. Fujikawa S. Freeze-fracture and etching studies on membrane damage on human erythrocyte caused by formation of intracellular ice. *Cryobiology* 1980;17(351-362).
14. Morris GJ, McGrath JJ. Intracellular ice nucleation and gas bubble formation in spirogyra. *Cryo-Letters* 1981;2:341-352.

15. Ashwood-Smith MJ, Morris GW, Fowler R, Appleton TC, Ashorn R. Physical factors are involved in the destruction of embryos and oocytes during freezing and thawing procedures. *Human Reproduction* 1988;3:795-802.
16. Farrant J. Water transport and cell survival in cryobiological procedures. *Phil Trans Royal Soc London B* 1977;278:191-205.
17. Meryman HT. Exceeding of a minimum tolerable cell volume in hypertonic suspensions as a cause of freezing injury. In: Wolstenholme GEWaOC, M., editor. *The Frozen Cell*. London: J. & A. Churchill; 1970. p. 51-67.
18. Meryman HT. Freezing Injury and Its Prevention in Living Cells. *Annual Review of Biophysics and Bioengineering* 1974;3:341-363.
19. Lovelock JE. The Haemolysis of Human Red Blood-Cells by Freezing and Thawing. *Biochimica Et Biophysica Acta* 1953;10(3):414-426.
20. Ebertz SL, McGann LE. Cryoprotectant permeability parameters for cells used in a bioengineered human corneal equivalent and applications for cryopreservation. *Cryobiology* 2004;49(2):169-180.
21. Acker J, McGann LE. Protective effects of intracellular ice during freezing? *Cryobiology* 2003;46:197-202.
22. Coticchio G, Bonu MA, Borini A, Flamigni C. Oocyte cryopreservation: a biological perspective. *European Journal of Obstetrics Gynecology and Reproductive Biology* 2004;115:S2-S7.
23. Acker JP, Larese A, Yang H, Petrenko A, McGann LE. Intracellular ice formation is affected by cell interactions. *Cryobiology* 1999;38(4):363-371.
24. Armitage WJ, Juss BK, Easty DL. Differing effects of various cryoprotectants on intercellular junctions of epithelial (MDCK) cells. *Cryobiology* 1995;32:52-59.
25. Armitage WJ, Juss BK. The influence of cooling rate on survival of frozen cells differs in monolayers and suspensions. *Cryo-Letters* 1996;17:213-218.
26. Acker J, Elliott JAW, McGann LE. Intercellular ice propagation: Experimental evidence for ice growth through membrane pores. *Biophysical Journal* 2001;81(3):1389-1397.
27. Yang H, Jia XM, Ebertz SL, McGann LE. Cell junctions are targets for freezing injury. *Cryobiology* 1996;33:672-673.

28. Acker JP, McGann LE. Cell-Cell Contact Affects Membrane Integrity after Intracellular Freezing. *Cryobiology* 2000;40:54-63.
29. Pegg DE. Cryopreservation of vascular endothelial cells as isolated cells and as monolayers. *Cryobiology* 2002;44(1):46-53.
30. McGann LE, Kruuv J, Frey HE. Repair of Freezing Damage in Mammalian-Cells. *Cryobiology* 1972;9(6):496-501.
31. Pascual G, Rodriguez M, Corrales C, Turegano F, Garcia-Honduvilla N, Bellon JM, et al. New approach to improving endothelial preservation in cryopreserved arterial substitutes. *Cryobiology* 2004;48(1):62-71.
32. Bujan J, Pascual G, Lopez R, Corrales C, Rodriguez M, Turegano F, et al. Gradual thawing improves the preservation of cryopreserved arteries. *Cryobiology* 2001;42(4):256-265.
33. Langerak SE, Groenink M, van der Wall EE, Wassenaar C, Vanbavel E, Van Ball MC, et al. Impact of current cryopreservation procedures on mechanical and functional properties of human aortic homografts. *Transplant International* 2001;14(4):211-280.
34. Routledge C, Armitage WJ. Cryopreservation of cornea: a low cooling rate improves functional survival of endothelium after freezing and thawing. *Cryobiology* 2003;46(3):277-283.
35. Zieger MAJ, Tredget EE, McGann LE. Cryomicroscopy of an in situ cell model of skin. *Cryo-Letters* 1997;18:117-126.
36. Lehle K, Hoenicka M, Jacobs VR, Schmid FX, Birnbaum DE. Cryopreservation of human endothelial cells for vascular tissue engineering. *Cryobiology* 2005;50(2):154-161.
37. Joyce NC, Harris DL, Zieske JD. Mitotic inhibition of corneal endothelium in neonatal rats. *Investigative Ophthalmology & Visual Science* 1998;39(13):2572-2583.
38. Stiemke MM, McCartney MD, Cantucrouch D, Edelhauser HF. Maturation of the Corneal Endothelial Tight Junction. *Investigative Ophthalmology & Visual Science* 1991;32(10):2757-2765.
39. Canals M, Costa-Vila J, Potau JM, Merindano MD, Ruano D. Morphological study of cryopreserved human corneal endothelium. *Cells Tissues Organs* 1999;164(1):37-45.
40. Ruoslahti E. Integrins. *Journal of Clinical Investigation* 1991;87(1):1-5.

41. Luchetti F, Mannello F, Canonico B, Battistelli M, Burattini S, Falcieri E, et al. Integrin and cytoskeleton behaviour in human neuroblastoma cells during hyperthermia-related apoptosis. *Apoptosis* 2004;9(5):635-648.
42. Webb DJ, Parsons JT, Horwitz AF. Adhesion assembly, disassembly and turnover in migrating cells - over and over and over again. *Nature Cell Biology* 2002;4:E97 - E100.
43. Frisch SM, Ruoslahti E. Integrins and anoikis. *Current Opinion in Cell Biology* 1997;9(5):701-706.
44. Short SM, Talbott GA, Juliano RL. Integrin-mediated signaling events in human endothelial cells. *Molecular Biology of the Cell* 1998;9(8):1969-1980.
45. Grossmann J. Molecular mechanisms of "detachment-induced apoptosis-Anoikis". *Apoptosis* 2002;7(3):247-260.
46. Hug TS. Biophysical methods for monitoring cell-substrate interactions in drug discovery. *Assay and Drug Development Technologies* 2003;1(3):479-488.
47. Hetzel FW, Kruuv J, McGann LE, Frey HE. Exposure of Mammalian-Cells to Physical Damage - Effect of State of Adhesion on Colony-Forming Potential. *Cryobiology* 1973;10(3):206-211.
48. McGann LE, Kruuv J, Frey HE. Effect of hypertonicity and freezing on survival of unprotected synchronized mammalian cells. *Cryobiology* 1972;9:107-111.
49. Gimbrone MA, Cotran RS, Folkman J. Human Vascular Endothelial Cells in Culture - Growth and DNA-Synthesis. *Journal of Cell Biology* 1974;60(3):673-684.
50. Yang HY, Acker J, Chen A, McGann L. In situ assessment of cell viability. *Cell Transplantation* 1998;7(5):443-451.
51. Jomha NM, Anoop PC, Elliott JAW, Bagnall K, McGann LE. Validation and reproducibility of computerised cell-viability analysis of tissue slices. *Bmc Musculoskeletal Disorders* 2003;4:-.
52. Turner T. In: Kluthe K, editor. Edmonton, AB; 2005.
53. Bovolenta C, Pilotti E, Mauri M, Turci M, Ciancianaini P, Fiscicaro P, et al. Human T-cell leukemia virus type 2 induces survival and proliferation of CD34(+) TF-1 cells through activation of STAT1 and STAT5 by secretion of interferon-gamma and granulocyte macrophage-colony-stimulating factor. *Blood* 2002;99(1):224-231.

54. Turzanski J, Grundy M, Shang SL, Russell N, Pallis M. P-glycoprotein is implicated in the inhibition of ceramide-induced apoptosis in TF-1 acute myeloid leukemia cells by modulation of the glucosylceramide synthase pathway. *Experimental Hematology* 2005;33(1):62-72.
55. Yang H, Acker JP, Cabuhat M, McGann LE. Effects of incubation temperature and time after thawing on viability assessment of peripheral hematopoietic progenitor cells cryopreserved for transplantation. *Bone Marrow Transplantation* 2003;32(10):1021-1026.
56. Wu XY, Cornellbell A, Davies TA, Simons ER, Trinkausrandall V. Expression of Integrin and Organization of F-Actin in Epithelial-Cells Depends on the Underlying Surface. *Investigative Ophthalmology & Visual Science* 1994;35(3):878-890.
57. Podesta F, Roth T, Ferrara F, Cagliero E, Lorenzi M. Cytoskeletal changes induced by excess extracellular matrix impair endothelial cell replication. *Diabetologia* 1997;40(8):879-886.
58. Meredith JE, Fazeli B, Schwartz MA. The Extracellular-Matrix as a Cell-Survival Factor. *Molecular Biology of the Cell* 1993;4(9):953-961.
59. Mettouchi A, Klein S, Guo WJ, Lopez-Lago M, Lemichez E, Westwick JK, et al. Integrin-specific activation of Rac controls progression through the G(1) phase of the cell cycle. *Molecular Cell* 2001;8(1):115-127.
60. Heilshorn SC, DiZio KA, Welsh ER, Tirrell DA. Endothelial cell adhesion to the fibronectin CS5 domain in artificial extracellular matrix proteins. *Biomaterials* 2003;24(23):4245-4252.
61. Wusteman M, Wang LH. Some observations on the use of cultured corneal endothelial cells as a model for intact corneal endothelium. *Cryobiology* 2000;40(4):376-380.
62. Acker J. Innocuous intracellular ice improves survival of frozen cells. *Cell Transplantation* 2002;11(6):563-571.
63. Ebertz SL. Cryobiology of human corneal cells [Ph. D.]. Edmonton: University of Alberta; 2002.
64. McGann LE. Differing actions of penetrating and nonpenetrating cryoprotective agents. *Cryobiology* 1978;15:382-390.

65. Muldrew KB, Hurtig M, Novak K, Schachar N, McGann L. Localization of Freezing Injury in Articular Cartilage. *Cryobiology* 1994;31:31-38.
66. Neronov A, Mazgalova J, Cholakova M, Dimitrova M, Deligiozova I, Kovatcheva S, et al. Integrity of endothelium in cryopreserved human cornea. *Cryoletters* 2005;26(2):131-136.
67. Schafer AT, Korber C, Scheiwe MW, Rau G, Franke P, Mittermayer C. Preliminary Investigation of Osmotic Properties and Freezing Behavior of Human-Endothelial Cells. *Cryo-Letters* 1986;7(1):55-67.
68. Pascual G, Jurado F, Rodriguez M, Corrales C, Lopez-Hervas P, Bellon JM, et al. The use of ischaemic vessels as prostheses or tissue engineering scaffolds after cryopreservation. *European Journal of Vascular and Endovascular Surgery* 2002;24(1):23-30.
69. Hornung J, Muller T, Fuhr G. Cryopreservation of anchorage-dependant mammalian cells fixed to structured glass and silicon substrates. *Cryobiology* 1996;33:260-270.
70. Feneberg W, Aepfelbacher M, Sackmann E. Microviscoelasticity of apical cell surface of human umbilical vein endothelial cells (HUVEC) within confluent monolayers. *Biophysical Journal* 2004;87:1338-1350.
71. Daw A, Farrant J, Morris GJ. Membrane leakage of solutes after thermal shock or freezing. *Cryobiology* 1973;10:126-133.
72. Farrant J, Morris GJ. Thermal Shock and Dilution Shock as Causes of Freezing Injury. *Cryobiology* 1973;10(2):134-140.
73. Morris GJ, Farrant J. Effects of Cooling Rate on Thermal Shock Hemolysis. *Cryobiology* 1973;10(2):119-125.
74. Tenchini ML, Bolognani L, Decarli L. Effect of hypertonicity on survival of unprotected human cultured-cells following freezing and thawing. *Cryobiology* 1980;17(2):120-124.
75. Zeng WX, Shimada M, Isobe N, Terada T. Survival of boar spermatozoa frozen in diluents of varying osmolality. *Theriogenology* 2001;56(3):447-458.
76. Jacobsen IA, Pegg DE. Cryopreservation of Organs : A Review. *Cryobiology* 1984;21:377-384.

77. Neronov A, Giurov P, Cholakova M, Dimitrova M, Neronciv A. Cryoprotection of porcine cornea: a scanning electron microscopy study. *Veterinari Medicina* 2005;50(5):219-224.
78. Stefanovich P, Ezzell RM, Sheehan SJ, Tompkins RG, Yarmush ML, Toner M. Effects of Hypothermia on the Function, Membrane Integrity, and Cytoskeletal Structure of Hepatocytes. *Cryobiology* 1995;32(4):389-403.